Coupling the regional climate model ICON-CLM v2.6.6 into the Earth system ~~framework~~model GCOAST-AHOI v2.0 using ~~the~~ OASIS3-MCT ~~coupler~~v4.0

Ha Thi Minh Ho-Hagemann[1], Vera Maurer[2], Stefan Poll[3], Irina Fast[4]

[1]Institute of Coastal Research, Helmholtz-Zentrum Hereon, Geesthacht, Germany (Ha.Hagemann@hereon.de)

[2]Deutscher Wetterdienst, Offenbach, Germany

[3] Institute of Bio and Geosciences Agrosphere (IBG-3), Forschungszentrum Jülich, Jülich, Germany; CASA-SDL Terrestrial Systems, Jülich Supercomputing Centre (JSC), Jülich, Germany

[4]German Climate Computing Center (DKRZ), Hamburg, Germany

Correspondence to: Ha Thi Minh Ho-Hagemann, Ha.Hagemann@hereon.de

Abstract

Interactions and feedback between compartments of the Earth system can have a significant impact on local and regional climate and its changes due to global warming. These effects can be better represented by regional Earth system models (RESMs) than by traditional stand-alone atmosphere and ocean models. Here, we present the RESM GCOAST-AHOI version 2.0, which includes a new atmospheric component, the regional climate model ICON-CLM, which is coupled with the ocean model NEMO and the hydrological discharge model HD via the OASIS3-MCT coupler. The GCOAST-AHOI model has been developed and applied for climate simulations over the EURO-CORDEX domain. Two 11-year simulations from 2008-2018 of the uncoupled ICON-CLM and GCOAST-AHOI give similar results for seasonal and annual means of near-surface air temperature, precipitation, mean sea level pressure and wind speed at 10 m height. However, GCOAST-AHOI has a cold SST bias of 1-2 ~~degrees c~~CK over the Baltic and the North Seas, most pronounced in winter and spring seasons. A possible reason for the cold SST bias could be the underestimation of the downward shortwave radiation at the surface of ICON-CLM with the current model settings. Despite ~~of~~ the cold SST bias, GCOAST-AHOI was able to capture other key variables such as those mentioned above well. Therefore, GCOAST-AHOI can be a useful tool ~~to apply~~ for long-term climate simulations over the EURO-CORDEX domain. Compared with the stand-alone NEMO3.6 forced by ERA5 and ORAS5 boundary forcing, GCOAST-AHOI has positive biases in sea ice fraction and salinity, but negative biases in runoff, ~~and discharge~~ which need to be further ~~s a more~~ investigated in the future to ~~further~~ improve the coupled simulations. The new OASIS3-MCT coupling interface OMCI implemented in the ICON-CLM model adds a possibility to couple ~~makes the~~ ICON-CLM ~~model more flexible to couple~~ with an external ocean model and an external hydrological discharge model using OASIS3-MCT instead of the YAC coupler. Using OMCI, it is also possible to set up a RESM with ICON-CLM and other ocean and hydrology models possessing the OASIS3-MCT interface for other regions, such as the Mediterranean Sea.

Keyword: GCOAST, ICON-CLM, OASIS3-MCT coupling interface, climate simulations, EURO-CORDEX, RESM

1 Introduction

GCOAST (Geesthacht Coupled cOAstal model SysTem) is an Earth system framework developed at Helmholtz-Zentrum Hereon, Germany (Staneva et al., 2018). GCOAST is a modular system of different models each developed for a specific component of the Earth system. Based on a specific scientific question, different models from GCOAST can be selected. These models can be plugged together by various couplers, such as OASIS3-MCT (Valcke et al., 2015), ESMF (Earth System Modeling Framework; Hill et al., 2004), or FABM (Framework for Aquatic Biogeochemical Models; https://fabm.net). The coupling can be done at different levels of coupling granularity and the couplers handle the exchange of information between model combinations, individual models, and processes.

GCOAST systems have been applied for several studies covering the Baltic and-North Sea region and part of the North Atlantic. These studies include atmosphere-river-ocean-sea ice coupling (Ho-Hagemann et al., 2020), atmosphere-wave coupling (Wahle et al., 2017; Wiese et al., 2019, 2020), wave-ocean coupling (Staneva et al., 2016; Schloen et al., 2017; Lewis et al., 2019), hydrosphere-biosphere coupling for the Elbe estuary (Pein et al., 2019), the total organic carbon-macrobenthos coupling model (Zhang et al., 2019), and multi-model couplings developed by Lemmen et al. (2018), which have been applied to assess ecosystem impacts of offshore wind farms (Slavik et al., 2019).

So far, the atmospheric model component of GCOAST has been the non-hydrostatic limited area atmospheric model COSMO-CLM v5.0 (Rockel et al., 2008). The COSMO (cOnsortium for Small-scale mOdeling) model was initially developed by the Deutscher Wetterdienst (DWD, the German Meteorological Service) in the 2000s as a limited-area weather forecast model. Later, it was further developed in the Climate Limited-area Modeling Community (CLM-Community) as the regional climate model COSMO-CLM (hereafter referred to as CCLM). In December 2021, ~~the~~ COSMO v6.0 was released which is the last version of the COSMO model. With this release, the development of the COSMO model ended after more than two decades. The successor of the COSMO model is the ICON model.

In 2001, a cooperation between the DWD and the Max-Planck Institute for Meteorology (MPI-M) was initiated, with the aim of developing a new modelling system for weather prediction and climate simulations. As one result of this initiative, the global numerical weather prediction model ICON (Icosahedral Nonhydrostatic) was developed (Zängl et al., 2015). Nowadays, with contributions from the Karlsruhe Institute of Technology (KIT) and the German Climate Computing Center (DKRZ), etc., the ICON Earth system framework ~~ICON-ESM~~ can include not only the atmospheric, land, river

routing, ocean-sea ice, wave, and biogeochemical compartments but also the Aerosols and Reactive Trace gases (ART) model. ICON can be set up to operate on several high-performance computing systems such as Bull ATOS at DKRZ (Hamburg, Germany), NEC-Aurora Tsubasa at DWD (Offenbach, Germany) or BullSequana at Forschungszentrum Jülich (FZJ, Jülich, Germany). ICON can be used on a wide range of scales from climate projection, climate prediction and numerical weather prediction down to large-eddy simulations (Dipankar et al., 2015; Heinze et al., 2017).

~~In addition to the main components of the climate system, ICON uses YAC (Yet Another Coupler; Hanke et al., 2016) to couple them.ICON can also be used in a configuration with regional grid refinement (2-way nesting) or in limited area mode.~~

The ~~In general~~atmospheric component of ICON~~,~~ includes two different physics packages ~~are available in ICON~~: the first one is the Numerical Weather Physics package of DWD (i.e. the ICON-NWP model); and the second one is the ECHAM physics package of MPI-M (i.e. ~~. In the second package,~~ the ~~global atmospheric model~~ ICON-A model, ~~(~~Giorgetta et al., 2018). The global atmospheric model ICON-A is coupled with the global ocean model ICON-O (Korn, 2017) and the land and biosphere model JSBACH (Reick et al., 2021) within the ICON Earth System Model (ICON-ESM; Jungclaus et al., 2022). ~~ICON can also be used for large-eddy simulations (Dipankar et al., 2015).~~ ICON-NWP can be also coupled with ICON-O in the ICON-Seamless Earth system coupling framework which has been newly developed during the recent~~for several~~ years. In ICON-Seamless, there are two options for the land surface schemes, TERRA and JSBACH, which are coupled via subroutine to the atmospheric component. A new land surface model (ICON-Land) is being developed based on JSBACH and some features of TERRA. Another component of ~~the~~ ICON-Seamless is the wave model ICON-Wave. The hydrological discharge model HD can now be used as an external model instead of being coupled as a subroutine of JSBACH.

The components of ICON are coupled together using YAC (Yet Another Coupler; Hanke et al., 2016). However, coupling between ICON components, or the coupling of multiple ICON components to an external model without a YAC coupling interface is not supported ~~and potentially impossible~~due to how the initial communicator splitting is implemented.

~~ICON can also be used for large-eddy simulations (Dipankar et al., 2015).~~ ICON can also be used in a configuration with regional grid refinement (2-way nesting) or in limited area mode. ICON-LAM is the Limited-Area Mode of ICON-NWP. Starting in 2017, DWD and the CLM-Community decided to develop the climate limited area mode (ICON-CLM, Pham et al., 2021) based on ICON-LAM.

~~Nowadays, with contributions from the Karlsruhe Institute of Technology (KIT) and the German Climate Computing Center (DKRZ), the ICON-ESM can include not only the atmospheric, land, river~~

~~routing, ocean-sea ice and biogeochemical compartments but also the Aerosols and Reactive Trace gases (ART) model. ICON can be set up to operate on several high-performance computing systems such as Bull ATOS at DKRZ (Hamburg, Germany), NEC-Aurora Tsubasa at DWD (Offenbach, Germany) or BullSequana at Forschungszentrum Jülich (FZJ, Jülich, Germany). ICON can be used on a wide range of scales from climate projection, climate prediction and numerical weather prediction down to large-eddy simulations (Heinze et al., 2017). In addition to the main components of the climate system, ICON uses YAC (Yet Another Coupler; Hanke et al., 2016) to couple them.~~ Within ~~the~~ ICON-Seamless, a limited area mode of the ocean model (ICON-O-LAM) is being developed and can be coupled with ICON-LAM via YAC.

As mentioned above, coupling a component or multiple components of ICON to an external model ~~which~~that has no YAC coupling interface is not supported and potentially impossible. For the~~To~~ coupling of~~e~~ ICON-CLM as an atmosphere component into GCOAST-AHOI, which includes HD and

~~To couple ICON to an external~~the ocean model ~~such as the~~ NEMO ~~model~~ (Nucleus for European Modelling of the Ocean, Madec et al. 2017), ~~which~~ represent~~s~~ing the ocean and sea ice components, basically, ~~within GCOAST,~~ there were two feasible options: either to implement a YAC interface~~s~~ in NEMO and HD, or to implement an OASIS interface~~s~~ in ICON-CLM. For the option one, the YAC coupling interface was added into the HD source code by M. Hanke (DKRZ) (see Hagemann et al. 2023), but YAC has~~is~~ not yet been available in the NEMO source code. ~~On~~To our current knowledge, there ~~has been~~ is no RESM with NEMO using the YAC coupler. The NEMO model is already linked to the OASIS coupler, which ~~can~~has been used to couple NEMO with many other model components. ~~To i~~Implementing the YAC interface in NEMO~~, it~~ would require a larger effort,~~take us a longer time~~ as the NEMO source code is much more complicated than the HD code. In ~~addition~~addition,~~On the other hand~~ although the NEMO source code is freely available, we are ~~normal~~ordinary users in the NEMO community, not ~~a~~ members of the model development team. Therefore, ~~Implementing~~ implementing and especially maintaining the YAC interfaces ~~within~~ in NEMO is a ~~major~~ big challenge. For the second option ~~two~~, HD and NEMO already have the OASIS3-MCT coupling interface (OMCI), so all we ~~only need~~had~~ve~~ to do was~~is~~ to ~~to~~ implement OMCI in ICON. Here, we also have the~~With an~~ advantage that we belong to the ICON development team of the CLM-Community, so that we can ~~reach~~get great and quick technical support ~~when coding with ICON~~ from the development team when coding with ICON. ~~The NEMO model is already linked to the OASIS coupler, which can be used to couple with many other model components. There is no obvious need for YAC interfaces in the NEMO users and developers community.~~ Therefore, in 2021, ~~it~~ we ~~was decided~~started to ~~to~~ port~~ing~~

the OASIS coupling interfaces from CCLM to ICON--CLM for the to coupleing withto NEMO and HD.

For Some other groups were using a similar method while coupling ICON into their available coupled system model which does n'ot haveinclude the YAC coupler. For example, regional ocean-atmosphere coupling over the Baltic Sea, Bauer et al. (2021) have implemented the ESMF interfaces in an earlier version of ICON-NWP as well as into the ocean model GETM to build up the regional ocean-atmosphere coupling over the Baltic Sea. However, they did not consider sea ice in the coupling. There is an ongoing work at FZJ to couple ICON-CLM with the Community Land Model (CLM) via the OASIS3-MCT coupler (manuscript in preparation). ICON-O is the global ocean model of the ICON family and could potentially replace NEMO within GCOAST, but it is not yet available as a regional ocean model for coupling with ICON-CLM.

ICON-NWP/ICON-CLM already includes the land surface schemes TERRA and JSBACH, which are coupled via subroutine to the atmospheric component. However, it might be desirable to couple with other land surface models such as the Community Land Model (CLM), as has been done for the CCLM via the OASIS interface (see Shrestha et al., 2014; Will et al., 2017). There is an ongoing work at FZJ to couple ICON-CLM with the Community Land Model (CLM) via the OASIS3-MCT coupler (in preparation).

The aim of this article is to give a detailed description of the OASIS3-MCT coupling interface (hereafter referred to as OMCI) in ICON-CLM (ICON release version 2.6.6), how to implement OMCI with as little modification of the ICON source code as possible, how to compile it on the high-performance computing system Levante at DKRZ, and how to run the coupled system model GCOAST-AHOI with ICON-CLM for climate simulations over the EURO--CORDEX domain. This information is useful to other groups planning to couple ICON-CLM with NEMO or any other ocean model that already has an available OASIS3--MCT interface available. The Earth System Modelling (ESM) Community agrees that ICON and IFS (coupled to FESOM and NEMO) will play a central role within the Helmholtz Association of German Research Centres (HGF). This new OMCI opens more opportunities to use ICON-CLM in ESM applications as well as in other modelling communities. The OMCI can also be applied to couple with a land surface model with minor necessary adaptations.

We briefly introduce the coupled system model GCOAST-AHOI in Section 2, and2 and describe the details of OMCI in ICON-CLM in Section 3. Experiment setups are presented in Section 4, followed by an analysis of the model simulations in Section 5. Finally, conclusions and a discussion are given in Section 6.

2 The coupled system model GCOAST-AHOI

GCOAST-AHOI is a subset of GCOAST that includes model components for **A**-Atmosphere and Land, **H**-Hydrological discharge, **O**-Ocean, and **I**-Sea Ice. GCOAST-AHOI version 1.0 (Ho-Hagemann et al., 2020) contains the atmospheric model CCLM v5.0, the ocean model NEMO v3.6 (including the sea ice model LIM3) and the hydrological discharge model HD v4.0 (Hagemann and Dümenil, 1998; Hagemann et al., 2020), coupled via OASIS3-MCT v2.0. A detailed description of CCLM, NEMO and HD as components of GCOAST-AHOI can be found in Ho-Hagemann et al. (2020).

In the GCOAST-AHOI version 2.0, ICON-CLM replaces CCLM as atmospheric model, which is coupled to NEMO v3.6 and HD v5.1 via OASIS3-MCT v4.0. By coupling the atmosphere-ocean-river runoff models in GCOAST-AHOI, we aim to close the water balance in the RESM. Figure 1 illustrates the three models exchanging radiation, wind, pressure, temperature, humidity, water, and sea ice related variables at their interfaces via the OASIS coupler.

The OMCI in NEMO v3.6 has been modified compared to the original one in the officially released version at http://forge.ipsl.jussieu.fr/nemo/wiki/Users/release-3.6 to be able to receive state variables from the atmospheric model (Ho-Hagemann, 2024). Supplement S1 contains a flowchart of the OMCI for NEMO v3.6. This flowchart differs slightly from Figure 9 in Will et al. (2017), who used the older version NEMO v3.3. The OMCI in HD can be found in the source code publication of Hagemann and Ho-Hagemann (2021) and Hagemann et al. (2023). Supplement S2 shows the OMCI of HD. In this article, we describe in detail the OMCI in ICON-CLM~~, or ICON for short~~.

In Section 3, we demonstrate the construction of the OMCI in ICON-CLM and the optional coupling methods between ICON-CLM and NEMO.

3 The coupling OASIS3-MCT interface in ICON

3.1 Interface structure

Figure 2 shows a flowchart of ICON with the OMCI implemented for coupling with NEMO and HD. 10 levels of ICON's source code are described: the first level is the main program ICON, the second level starts with the *start_mpi*, then *atmo_model* and ends with *stop_mpi*, etc.

Levels 2 to 6, 8 and 9 comprise subroutines of ICON (marked in red) that are modified by the coupling. On levels 3 to 7 and 10, new subroutines (orange boxes B1-B7) have been added with the OMCI. They are organized in three modules (cpl_oas_vardef.f90, cpl_oas_mpi.f90 and cpl_oas_interface.f90) containing about 3000 lines of Fortran code (including the current debug lines). The files have been added to the icon/externals/oasis3-mct directory and linked to the src/atm_phy_nwp directory of the ICON source tree. The detailed description of the interface

structure can be found in Supplementary S4.

Supplement S54 contains a guide for compiling ICON with this OMCI on Levante at DKRZ. The preparation of OASIS input files for GCOAST-AHOI is described in Supplement S5S6, which is accompanied by an example of the namcouple file in Supplement S76 and the namelist_cpl_atm_oce in Supplement S87. The command to run GCOAST-AHOI on Levante is provided in Supplement S98. The complete package to conduct experiments for this study is included in the Starter Package for ICON-CLM Experiments (SPICE; Rockel and Geyer, 2022), which is a workflow engine to easily perform long-term simulations. This tool has been further developed from the ICON-CLM_SP starter package (Pham et al. 2021). Some additional parts for coupling with NEMO and HD have been added to the original package.

3.2 Coupling methods

In the officially released version of NEMO v3.6, several fluxes and variables, including shortwave (SW) and longwave (LW) radiation fluxes, latent (LH) and sensible heat (SH) fluxes, rain, snow, evaporation, ice sublimation, mean sea level pressure (MSLP) and surface momentum, can be sent from an atmospheric model to NEMO via the OASIS3-MCT coupler. To be able to receive state variables from the atmospheric model, the OMCI in NEMO v3.6 has been modified to allow air temperature and air specific humidity at 2 m height (T_2M and QV_2M respectively) to be sent from the atmospheric model to NEMO. This allows NEMO to use these variables to calculate the LH and SH, as in the case of the stand-alone NEMO using the "CORE bulk formulae" (Large and Yeager, 2004). Thus, we have three options for the coupling method between ICON and NEMO:

a) CPL_flx: **flux coupling**, which is the default option in the NEMO source code (described above)
b) CPL_var: **state variable coupling**, the new method, where SW and LW, T_2M, QV_2M, wind speed at 10 m height (UV_10M), rain, snow, MSLP, and surface momentum are sent from ICON-CLM to NEMO. NEMO calculates LH and SH using the "CORE bulk formulae" which is based on the Monin Obukhov similarity theory.
c) CPL_mix: **mixture coupling**, the new method, like CPL_var, but ICON-CLM also sends LH and SH to NEMO. NEMO then averages them with the LH and SH calculated using the "CORE bulk formulae".

With the modification of OMCI in NEMO v3.6, it is now easy to select the coupling method via the namelist settings. Section 5 considers the simulations using the coupling method 3 (CPL_mix), which was also used in Ho-Hagemann et al. (2020). An extra experiment using the coupling method 1 (CPL_flx) is also conducted and analyzed in Section 5.

In turn, NEMO sends the sea surface temperature, sea ice fraction and sea ice albedo to ICON-

CLM. Fig. ure 3 illustrates how the surface temperature is updated in ICON over the ocean (left side) and over land (right side) in the presence of sea ice and snow. ICON utilizes a tile approach to compute surface fluxes of momentum and scalars. For the "sea-water type" grid boxes, the grid box mean fluxes are computed as a weighted average of the fluxes over ice and over open water, using the fractional ice cover *fice* and the fractional open water cover (*1 – fice*) as the respective weights. Sea ice in each ICON grid box is considered only if *fice* exceeds its minimum value of 0.015. Otherwise, the grid box is treated as ice-free. In ICON, two types of surface temperature are considered: the ground temperature t_g and the surface temperature t_s. If a grid box is covered by sea ice or snow, t_g is the mixed temperature of the free sea ice/free snow surface temperature and the temperature on top of the sea ice/snow. Under the sea ice, t_s is calculated as a mixture of the free sea ice temperature and the salt water freezing temperature of 271.45 K. If there is no sea ice or snow in the grid box, t_g is equal to t_s. In principle, NEMO can send the mixed sea ice and water temperature to ICON to update t_g over the ocean points, as in CCLM in Ho-Hagemann et al. (2020). Or it can send the open water temperature, the sea ice surface temperature and the sea ice fraction so that ICON can calculate t_g as the mixture. However, in the uncoupled mode of the current ICON-CLM version, the sea surface temperature (SST) forcing is read in as the variable t_seasfc (or t_s_w in Fig. 3) and passes through the subroutines *nwp_surface_init* and *process_sst_and_seaice* to calculate t_g. To be consistent with the ICON-CLM updates, we pass the SST (to update the t_seasfc), the sea ice fraction (to update fr_seaice), and the sea ice albedo (alb_si_ext) from NEMO to ICON. ICON will then calculate t_g, t_s, alb_si, etc. using its sea ice scheme. In the future, we may modify this coupling method by using the sea ice temperature from NEMO.

4 Experimental design

In this study, two four main experiments are conducted for the period of 2008-2018 (Table 2). with tThe uncoupled ICON (**ICON266**), the coupled and GCOAST-AHOI (**ICPL266**), the stand-alone NEMO v3.6 (**NEMO3.6**), and the stand-alone HD v5.1 forced by ICON266 runoffs (**HDICON266**)for the period of 2008-2018. One extra Two additional experiments are conducted: **ICPL266_noNewa** is conducted as a sensitivity test for the location of the Newa River mouth on NEMO grid, . Aandanother extra experiment **ICPL266_flx** is conductedto test the coupling method CPL_flx.

An Each experiment starts on 01 January 2008 and ends on 01 January 2019, restarting each month. The integration domains of ICON, NEMO and HD are displayed in Fig. 4. The namelist setup of physical parametrization for ICON-CLM is similar to that of the NUKLEUS project (B. Geyer,

personal communication). The resolution of ICON is R13B5, with an approximate mesh size of 12 km, using 60 vertical levels. The model top height is at 23.5 km. The following physical schemes are used in the current namelist setting of ICON: Radiation scheme ecRad (Hogan and Bozzo, 2018; Rieger et al., 2019); Mass-flux shallow and deep convection scheme (Tiedtke, 1989; Bechtold et al., 2008); Microphysics single-moment scheme (Doms et al., 2004); Planetary boundary layer scheme prognostic TKE (Raschendorfer, 2001; Raupach and Shaw, 1982); Land-surface scheme tiled TERRA (Schrodin and Heise, 2001; Schulz et al., 2016; Schulz and Vogel, 2020). The initial and lateral boundary forcing of ICON is obtained from the ERA5 reanalysis data (Hersbach et al., 2020). The Tegen aerosol climatology (Tegen, 1997), i.e. a monthly aerosol optical depth of sulphate droplets, total dust, organic carbon, black carbon, and sea salt, is used in this study. The initial and daily lateral boundary forcing of NEMO is taken from the ORAS5 reanalysis data (Copernicus Climate Change Service, 2021). The spatial resolution of NEMO is ~3.7 km with 50 vertical levels. In the stand-alone mode, NEMO3.6 is driven by the atmospheric ERA5 data, the ocean ORAS5 data and ~~the~~ climatology~~v~~ical river runoff data. HD has the resolution of 1/12 degrees, ca. 8 km. More information on the model configuration can be found in Table 1 and in Ho~~-~~-Hagemann et al. (2020).

To estimate the computational performance of the coupled model, we used LUCIA (Maisonnave and Caubel, 2014), which is part of OASIS3-MCT. In Supplement S10~~9~~ and Fig. S1, we describe how to use LUCIA for GCOAST-AHOI to optimize the computational performance.

5 Evaluation of ~~Model~~ model simulations

The first two years 2008-2009 are excluded as spin-up time, and the output data of the two simulations ICON266 and ICPL266 for nine years (2010-2018) are compared with the observational and the ERA5 reanalysis data to assess the model performance. For sea surface temperature (SST), we use the Operational Sea Surface Temperature and Ice Analysis (OSTIA) data (Good et al. 2020) to evaluate the simulated SST of ICPL266. For air temperature at 2 m height (T_2M) and precipitation (TOT_PREC), the daily E-OBS data (Haylock et al. 2008; Van den Besselaar et al. 2011) version 27.0 on the grid of 0.11 degree are used. The ERA5 reanalysis data are interpolated onto the E-OBS grid and used as a reference for comparison with the simulated shortwave and longwave surface radiation, turbulent~~ce~~ fluxes, mean sea level pressure (PMSL), wind speed at 10 m height (SP_10M), and T_2M. The Surface Radiation Data Set - Heliosat (SARAH) - Edition 2 (Pfeifroth et al. 2017) is used to evaluate the shortwave downward radiation of the simulations.

Seasonal means of winter (DJF), spring (MAM), summer (JJA), autumn (SON) and annual means (ANN) of several variables are ~~analysed~~analyzed~~.~~ ~~as following~~in this section.

5.1 Sea surface temperature and 2m air temperature

Over the ocean, the sea surface temperature (SST) of ICON266 is the ERA5 forcing data, which is based on observations, so it's very close to the OSTIA data (not shown). Thus, the SST difference between the coupled and the stand-alone ~~run~~ICON-CLM simulations (Fig. ~~6~~S2) can be interpreted as a bias towards a measurement-based product. In the coupled model, the SST is provided by NEMO over the GCOAST domain. In general, ICPL266 has a cold SST bias of about 1-3 ~~degrees~~ °C compared to OSTIA over the GCOAST domain, except around the British coast in summer (JJA, Fig. 5~~6~~a). The SST bias of ICPL266_flx (Fig. 5b) is similar to ICPL266 (Fig. 5a). Ho-Hagemann et al. (2020) not~~indicated~~ed that using ~~the~~ CPL_flx when coupling COSMO-CLM with NEMO leads to larger biases in the~~on~~ SST than using CPL_mix. This is not the case here when coupling ICON-CLM. A possible~~tential~~ reason for this is that due to the tile approach (cf. Sect. 3.2), the fluxes from ICON-CLM to NEMO are sent separately over water and sea ice, while COSMO-CLM v5.0 doesn't have the tile approach, therefore, the fluxes in each ocean grid box sent from the atmosphere ~~sent~~ to the ocean ~~is~~are the mixed fluxes of water and sea ice.

The annual mean SST bias of the stand-alone NEMO3.6 is less than 0.5 ~~degrees~~°C over the Baltic and North Seas, and of about -1 to -2 °C~~degrees~~ over the North Atlantic compared to the OSTIA data (Fig. 5c). In summer, ~~the~~a positive SST bias of about 1-2 °C~~degrees~~ is ~~found~~present over the Baltic and North Seas. ~~-~~In this case, the reduction of SST by the coupling reduces the warm bias of the stand-alone NEMO3.6.

The cold SST bias of ICPL266 over the GCOAST domain ~~may~~ intensif~~y~~ies the cold T_2M bias (Fig. 6~~7~~b, Fig. ~~S1~~S2b), especially in winter (DJF) and spring (MAM). In summer, ICPL266 reduces the warm T_2M bias of ICON266 (Fig. 6~~7~~a). In general, the annual (ANN) T_2M bias of ICPL266 is slightly ~~colder~~ more negative ~~(e.g.~~by about 0.5°C~~)~~ than that of ICON266. ICPL266_flx ~~simulates~~reproduces~~has~~ a similar T_2M (Fig. 6c) ~~simulation as~~to that of ICPL266. Comparison with the E-OBS data (Fig. S3~~2~~) shows similar results to Fig. 6~~7~~, except over ~~Nothern~~Northern Africa and Turkey, where the quality of the E-OBS data is affected by the lack of observations in that region (cf. Fig. 1 in Hagemann and Stacke, 2022).

5.2 Shortwave radiation, longwave radiation, and turbulent fluxes

A possible reason for the SST cold bias of ICPL266 may be that the shortwave and longwave radiation from ICON-CLM sent to NEMO is too low. Figure ~~S3~~ S4 shows the relative bias (%) of the shortwave downward radiation (SWDN) of ICON266 and ICPL266 compared to the ERA5 data, as well as the relative difference (%) between SARAH2 and ERA5. Figure 7~~8~~ shows a zoomed section of Fig. ~~S3~~ S4 over the GCOAST ocean domain (note the adapted ~~colour~~color scale). In general, both ICON266 and

ICPL266 have a positive SWDN bias of less than 10 % over land compared to ERA5, except for the larger bias of 15-20 % over northern Europe in winter and eastern Europe in autumn (Fig. ~~S3~~S4). Over the North Sea, ICON266 and ICPL266 have a small negative bias of about 5-10 % compared to ERA5 (Fig. 7~~8~~). The area of negative SWDN bias in the North Sea is slightly larger in ICPL266 than in ICON266. Comparing the ERA5 data and the SARAH2 data, SWDN over southern Europe is similar between the two datasets, with SARAH2 being slightly larger over land (Fig. S4~~3~~). In general, the SWDN of ICON266 and ICPL266 over the North Sea is rather close to the SARAH2 data, but slightly overestimated over the Baltic Sea.

Figure ~~S4~~ S5 in the Supplementary Appendix shows a similar plot to Fig. S4~~3~~, but for the longwave downward radiation (LWDN) and without the SARAH2 data, as it is not available. The modeled LWDN has a negative bias of about 2-4 % annually and a larger bias in winter of about 6-8 %, most pronounced over land. Over the ocean, ICON266 reproduces well the LWDN of the ERA5 data, and ICPL266 has a small negative bias of 2-4 %. Overall, the negative SWDN bias over the North Sea and the negative LWDN bias of ICON-CLM give an indication why the ICPL266 shows an increased cold SST bias.

The ERA5 reanalysis data is used as the atmospheric forcing for the uncoupled NEMO3.6, and ~~The~~ the namelist settings of the NEMO model used in this study were tuned ~~to the ERA5 forcing data in the uncoupled mode~~for an SST close to OSTIA~~. The annual mean SST bias of the stand-alone NEMO is less than 0.5 degrees over the Baltic and North Seas, and of about -1 to -2 degrees over the North Atlantic compared to the OSTIA data (not shown). In summer, the positive SST bias of about 1-2 degrees is found over the Baltic and North Seas~~ (Fig. 5c) ~~(not shown)~~. If ~~using~~ the same namelist settings of NEMO3.6 are used for ICPL266, ~~In the future,~~ to reduce the cold SST bias over the North Sea in the coupled simulations, a bias correction for SWDN and LWDN should be done. Figures S6a, b and Figures S7 a, b show the seasonal SWDN and LWDN of ICPL266 and NEMO3.6 averaged over the North Sea and Baltic Sea ~~are shown~~ for the period of 2010-2018~~ are shown~~. Note that we don't show the result of ICPL266_flx in Figs. S6 and S7 because there is no output of LWDN in ICPL266_flx due to the setup of the CPL_flx coupling method. Over the North Sea, the SWDN of ICPL266 is smaller than the ERA5 used for NEMO3.6 in spring and summer (Fig. S6a), which ~~that~~ mainly leads to ~~for~~ the cold SST bias of ICPL266 (Fig. 5a). Therefore, we plan to increase the SWDN of ICON by about 10 % before sending it to NEMO. However, the cold SST bias over the Baltic Sea does not seem to be directly related to the SWDN ~~and LWDN~~as there is no clear SWDN difference between ICPL266 and NEMO3.6 in summer or in any other season (Fig. S6a). The LWDN of ICPL266

is similar to NEMO3.6 in summer but slightly smaller in the other three seasons, both over the North Sea and the Baltic Sea. Increasing the LWDN in ICON-CLM by about 5-10 W/m2 before sending it to NEMO ~~will~~should be tested to reduce the SST bias. Note that the seasonal cycle of LWDN is more pronounced over the North Sea than over the Baltic Sea.

We also compare the turbulent heat flux (i.e. the sum of SH and LH) of NEMO3.6 and the flux of NEMO in ICPL266, averaged over the North Sea and the Baltic Sea (Fig. S6c and Fig. S7c), and the~~ir~~ net downward heat flux~~es~~, which is the sum of SWDN, LWDN, SH and LH (Fig. S6d and Fig. S7d). We only consider~~show only~~the turbulent flux because NEMO doesn't write out SH and LH ~~in the output~~ separately, but only the SWDN, LWDN and the net downward heat flux~~es~~. Note that the turbulent flux from NEMO3.6 is calculated using the "CORE bulk formulae", and due to the CPLmix coupling method used, the turbulent flux in NEMO from ICPL266 is the average of the flux from ICON-CLM and the one calculated inside NEMO (see section 3.2). The results are similar for both seas. The turbulent flux and the net downward flux of the two experiments are quite similar with the largest differences in winter (DJF) and summer (JJA).

Using ERA5 as a reference, the SH and LH biases of ICON266 and ICPL266 are shown in Fig. S8 and Fig. S9. Over land, the bias of ICON266 is very similar to that of ICPL266. However, over the ocean, the bias of ICPL266 is generally more positive (i.e. the fluxes are less negative) than that of ICON266 with the largest bias over the North Atlantic. Smaller heat fluxes are consistent with lower SSTs in ICPL266, as lower SSTs lead to ~~higher~~~~greater~~larger stability and less vertical mixing. Over the North and Baltic Seas, SH and LH of ICPL266 are quite close to ERA5. Despite of the SST forcing from ERA5, ICON266 has a negative SH bias of about -5 to -15 W/m^2 over the North and Baltic Seas, especially in winter. This suggests a future analysis of the difference in air temperature at the lowest level of ICON-CLM and ERA5.

Besides the energy flux biases causing the cold SST bias~~The negative wind speed bias in ICPL266 (Fig. 9) could be another element contributing to the SST bias, which needs to be analyzed in more detail in the future. , Otherwise,~~ a ~~short~~ spin-up time of 2 years may be too short for NEMO to reach the stable state, leading to the cold SST bias. In addition, NEMO's namelist settings should also be optimized for the coupled simulations.

Currently, ~~In~~ in the COPAT2 (Coordinated Parameter Testing, phase 2) initiative of the CLM-Community, several parameters of ICON-CLM are being tested in a similar way as done for the COSMO-CLM model (Russo et al., 2024) to find out the recommended settings. For example, the use of the transient aerosol MAC2-SP (Kinne, 2019; Stevens et al., 2017) and a careful adjustment of various namelist settings related to cloud cover, the soil and vegetation scheme and the turbulent

transfer will further reduce the T_2M cold bias and improve the shortwave downward radiation.

5.3 Precipitation, mean sea level pressure, and wind speed

The precipitation biases (Fig. 9) of the ~~two~~ three simulations ICON266, ~~and~~ ICPL266 and ICPL266_flx compared to the E-OBS data are very similar in general, with a wet bias in winter and spring and a dry bias in summer (JJA) and autumn (SON~~, Fig. 10~~). Fig. ~~S5~~ S10 and Fig. S11~~6~~ in the Supplementary show the biases of PMSL and SP_10M of ICON266 and ICPL266 compared to ERA5. The PMSL and SP_10M figures of ICPL266_flx are not shown because they are very similar to those of ICPL266.

ICPL266 tends to overestimate the PMSL throughout the year except in the summer, while ICON266 has only a pronounced positive bias in winter (DJF) and negative bias in summer (JJA). The wind speed of the two simulations is very similar over land (Fig. S11). ICPL266 ~~tends to~~ reduces the wind speed over the GCOAST ocean domain by up to 1.5 m s^{-1} compared to ICON266 (Figs. 8, S11). Therefore, while ICON266 has a positive bias of about 0.5 m s^{-1} over the North Sea and the Baltic Sea in winter (Fig. S11a), ICPL266 is very close to ERA5 (Fig. S11b). In general, ICPL266 produces a cooler SST and weaker wind speed than ICON266, ~~that is~~ consistent with the smaller SH ~~as~~ mentioned above in Section 5.2. This positive feedback is known as the thermal feedback (TFB) mechanism in the atmosphere-ocean surface coupling process ~~between the atmosphere and ocean surface~~ (Zhang and Perrie, 2001; Renault et al., 2023).

Figure 10~~1~~ shows monthly climatologies~~y~~ of different variables (T_S, T_2M, TOT_PREC, PMSL) over the GCOAST domain or the whole EURO-CORDEX domain, considering only ocean or land points. ICPL266 has a cold T_S bias of about 1-2 °C ~~degrees~~ over the ocean (Fig. 10~~1~~a), which also causes the T_2M bias of 0.5-1 ~~degrees~~ °C over the ocean (Fig. 10~~1~~c). In winter, ICPL266 is slightly colder over land than ICON266 and E-OBS (Fig. 10~~1~~d). In summer, both simulations are very close to E-OBS. The simulated precipitation of ICON266 tends to be overestimated compared to E-OBS with a maximum in May and June, and slightly underestimated in August and September (Fig. 10~~1~~b). The coupled run shows 1-3 mm/month less precipitation than the atmosphere-only experiment. In previous studies by Ho-Hagemann et al. (2015, 2017), the stand-alone atmospheric model COSMO-CLM has a dry bias in summer and the coupled run reduces the dry bias due to the improvement of the moisture convergence and transport from ocean to land. This situation is not found in the current study, which needs to be thoroughly analyzed in the future.

For the PMSL, the whole EURO-CORDEX domain is considered, but separately for ocean points (Fig. 10~~1~~e) and land points (Fig. 10~~1~~f). In both cases, ICPL266 has a larger PMSL than ICON266. The higher surface pressure in ICPL266 may be caused by the cooler air near the surface (due to the

negative T_2M bias) which leads to a higher density of the air mass and therefore a higher pressure. Over the ocean, the PMSL of ERA5 is better reproduced by ICPL266 than by ICON266. Over land, ICPL266 increases the PMSL positive bias in winter compared to ICON266. ICPL266_flx and ICPL266 have similar results (not shown) indicating that the coupling methods used in GCOAST-AHOI v2.0 don't affect the simulated ~~the~~ climate variables strongly in this study.

5.4 Sea ice

The sea ice fraction bias of ICPL266 is about 0.2-0.3 over the Bothnian Bay and Sea in winter and spring (Fig. 11~~2~~a), while ICPL266_flx has a larger bias of about 0.3-0.5 (Fig. 11b) and the ERA5-forced NEMO3.6~~-~~ has a relatively small positive ice fraction bias there (Fig. 11~~2~~c~~b~~). The monthly mean sea ice fraction averaged over the Bothnian Bay and Sea from ICPL266 and NEMO3.6 compared to the OSTIA data is shown in Fig. ~~12c~~11d, where the sea ice temporal variation is quite well captured by the two models, with a high peak in spring 2010 and a low peak in spring 2015. However, all ~~both~~ three ~~models~~ simulations overestimate the sea ice fraction of OSTIA, with ~~ICPL266~~the two coupled simulations showing a larger positive bias also in the time series. While ICPL266 has a winter SWDN about 8 % larger than ERA5 (Fig. 7~~8~~b), the incoming shortwave radiation is relatively small over the high latitudes ~~regions~~ in winter. Therefore, we don't expect the positive SWDN bias to be the main reason for the overestimation of sea ice. However, the LWDN of ICPL266 is about 10 W/m^2 ~~less~~ lower than ERA5 (the forcing for NEMO3.6) in winter over the North and Baltic Seas (Figs. ~~S5b~~S6b, ~~S6b~~S7b), and T_2M is about 3 ^{o}C lower than ERA5 over the Scandinavian region surrounding the Bothnian Bay and Sea (Fig. 6~~7~~b). The cold T_2M bias and negative LWDN bias of ICPL266 may explain its positive sea ice fraction bias. The cold air temperature above the sea ice surface often ~~generates~~ produces more sea ice in winter and spring, especially over an area with water of low salinity, such as the Bothnian Bay and Sea. Figure 6c shows the larger T_2M cold bias of ICPL266_flx over the Baltic Sea in spring about 1^{o}C more than ICPL266 (Fig. 6b) which is consistent with the larger sea ice fraction bias of ICPL266_flx (Fig. 11b) compared with that of ICPL266 (Fig. 11a).

Another factor that could contribute to an increase in sea ice cover in spring would be an increase in river runoff, which would result in less salty sea water and therefore more sea ice. These two variables ~~will be~~are analyzed in the next section.

5.5 Salinity and river runoff

As mentioned in section 4, NEMO3.6 uses a climatological dataset for river runoff. Therefore, a rough verification of the river runoff produced by the HD model in ICPL266 can be made by comparing against this climatological river runoff ~~from NEMO3.6~~. Differences in sea surface salinity

and river runoff between ICPL266 and NEMO3.6 are shown in Figure~~.~~ ~~13~~12. The ~~ICPL266 simulated~~ salinity simulated by ICPL266 is about 0.3-1 PSU higher than that of NEMO3.6 along the British Isles and the North Sea coast, and about 0.9-1.8 PSU higher in the Baltic Sea. Two areas with the largest salinity differences of more than 2 PSU are found south of the Kattegat and in the Gulf of Finland (Fig. ~~13a~~12a). The river runoff differences (Fig. ~~13b~~12b) are largest near the Ems and Newa estuaries with more than 0.1 and 0.2 kg/m2/s, respectively. The small river runoff difference between the two models at Kattegat cannot be used to directly explain the increase in salinity there. The river runoff differences near the Ems estuary have opposite signs (blue ~~dot~~ point ~~overlain~~ overlaid by a red one in Fig. ~~13b~~12b), but very similar values. The reason for this may be~~-~~ the discrepancy ~~of~~ in the locations of river mouths ~~locations~~ between the NEMO3.6 setup, where the river runoff is taken from a climatology, and those in ICPL266, which are defined based on the river mouths in the HD model and the NEMO land-sea mask. In the latter case, the river mouths of the HD model are interpolated onto the NEMO grid by searching for the closest ocean point of NEMO. ~~Therefore~~For example~~, e.g.,~~ the Ems ~~river~~ River mouth in ICPL266 may not be ~~at~~ in the same ~~location~~ position as in the climatology data. This discrepancy would lead to a difference in salinity near the coast (see Fig. ~~13a~~12a). The extent of the effect on salinity in the deeper layers of the ocean in a longer-term simulation needs to be analyzed in the future.

The large difference in river runoff near the Newa estuary is also caused by a mismatch in the locations of the river mouths ~~locations~~. In this case, the mouth of the Newa ~~river~~ River ~~mouth~~ in the climatology data (60.1333°N, 29.888°E) is located slightly northwest of its "real" location (Wikipedia: 59.9453°N, 30.1708°E). The interpolation program used to define the mouths of the HD rivers on the NEMO grid, by searching for the closest ocean point ~~of~~ to the mouth of the HD rivers, ~~mouth~~ found the mouth of the Newa ~~river~~ River at (59.95835°N, 30.20825°E), which is very close to the "real" position and at the furthest grid point to the east in the Gulf of Finland. However, in the NEMO model, this eastern boundary point in the Gulf of Finland is masked as a buffer zone. Therefore, the discharge from HD to NEMO at this point in ICPL266_noNewa was ignored in the NEMO calculations, resulting in a lack of freshwater inflow to the Gulf of Finland in ICPL266 (Fig. ~~13a2~~12ba~~2~~) and consequently an increase in salinity (Fig. ~~13b2~~12a~~b~~2). The ICPL266 simulation with the Newa ~~river~~ River mouth located on the NEMO buffer zone is referred to ICPL266_noNewa in Figure~~.~~ ~~13~~12. To overcome the location deficiency, that the Newa ~~river~~ River mouth was shifted one grid point to the west on the NEMO grid to allow the large amount of river runoff to enter the Gulf of Finland in the coupled model. Therefore, the salinity difference of ICPL266 compared to NEMO3.6 is reduced (Fig. ~~13a1~~12a1) and the river runoff difference shows the shift of the river mouth instead of the missing

one (Fig. ~~13b1~~12b1). The ~~relocation~~ shift of the Newa ~~river~~ River mouth has little effect on the simulated atmospheric variables, but improves the simulated salinity in the Baltic Sea, which is important for ecosystem modelling when a marine biogeochemical or ecosystem model such as ECOSMO (Daewel and Schrum, 2013) is coupled with GCOAST-AHOI in the future.

Other river mouths in the Baltic Sea have river runoff differences of less than 1.4 kg/m^2/s ~~while~~ when comparing ICPL266 to NEMO3.6. In general, ICPL266 tends to simulate less river runoff than the climatology, leading to increased salinity there. The sources of the river runoff used for NEMO in ICPL266 are the surface and sub-surface runoffs from the land component in ICON-CLM that are transported to the ocean by HD. We applied the HD model to calculate the discharge using the ICPL266 and ICON266 surface and subsurface runoff (Table 3) to evaluate it against the discharge observation. The annual discharge difference of ICPL266 and HDICON266 in the Baltic Sea is about -11 %. However, HDICON266 with a discharge of 12449 m^3/s is about -20 % biased towards the HELCOM (Helsinki Commission; Svendsen and Gustafsson, 2022) value of 15676 m^3/s. Note that for Baltic Sea ocean models, the mean long-term bias of river runoff must be less than 7 % (Hagemann and Stacke, 2022). In the North Sea, ICPL266 discharge is ~~ca.~~about -4 % compared to HDICON266, which has an annual value of 6366 m^3/s. However, both models have a dry discharge bias compared to the OSPAR data (Farkas and Skarbøvik, 2021), ~~data~~ which is 9190 m^3/s.

The main driver of the ~~R~~runoff is ~~caused by~~ precipitation. Figure 9 shows that over Scandinavia, ICON266 has a wet bias of about 10-30 mm/month in spring and summer compared to the E-OBS data. Thus, even with the wet precipitation bias, ICON266 has a dry discharge bias. ~~There~~At the same time, ICPL266 precipitation ~~amount~~ is lower than for ICON266 in spring and summer, and therefore ~~is~~ closer to the E-OBS data (Fig. 9b). This difference in precipitation ~~difference~~ between ICPL266 and ICON266 explains the -11 % ~~discharge~~ difference ~~of~~in discharge ~~–11 %~~, which increases the dry discharge bias. ~~ICON266 has the wet precipitation bias but the dry discharge bias.~~ The ~~improvement~~reduction of the precipitation bias in ICPL266 leading to a larger discharge dry bias implies that a better simulation of precipitation compared to observations does not necessarily lead to a better runoff. We note ~~Hagemann et al. (2024) found~~ that ~~a discharge dry bias when using~~ the runoff from the atmosphere-only ICON-CLM has a general dry bias, which ~~that~~ can be ~~. They~~ attributed ~~it~~ to the respective parametrizations in the TERRA land surface scheme used in ICON-CLM (S. Hagemann, pers. communication, 2024). ~~In the future, t~~This dry discharge bias can be improved either by using the JSBACH land-surface model ~~JSBACH~~ in ICON-Seamless, or by applying a discharge bias correction developed by Hagemann et al. (2024).

~~Coming back~~~~To return~~In ~~s~~Section 5.4, it was ~~to the~~ speculated~~ion above~~ that an increase in river

runoff would lead to~~result in~~ less salin~~ity~~ sea water and therefore more sea ice over the Baltic Sea. In our study, ICPL266 ~~produc~~simulates ~~a~~too little river runoff, leading to increased ~~river runoff decrease and~~ salinity in the Baltic Sea, which would mean less sea ice. ~~increase, which actually counteracts the increased~~but a However, the sea ice fraction is increased ~~increase~~ compared to the ERA5-forced NEMO3.6. Thus, the main factor causing ~~of~~ the bias in the sea ice fraction ~~bias~~ seems to be the cold bias in the air temperature ~~cold bias above the~~over sea ice in the Baltic Sea in winter and spring (Fig. 6b and c).

Conclusion and Outlook

In the present study, we introduce the regional Earth system model (RESM) GCOAST-AHOI version 2.0, in which a new atmospheric component - the regional climate model ICON-CLM version 2.6.6 - is coupled with the ocean model NEMO version 3.6 and the hydrological discharge model HD version 5.1 via the OASIS3-MCT coupler version 4.0.

GCOAST-AHOI v2.0 is developed and applied for climate simulations over the EURO-CORDEX domain. ~~Two~~ Several 11-year simulations from 2008-2018 of the uncoupled ICON-CLM (ICON266) and GCOAST-AHOI (ICPL266, ICPL266_flx, ICPL266_noNewa) yield similar results for seasonal and annual means of near-surface air temperature and precipitation, as well as mean sea level pressure and wind speed at 10 m height. However, ~~ICPL266~~ GCOAST-AHOI has a cold SST bias of 1-2 °C ~~degrees~~ over the Baltic and the North Seas, most pronounced in winter and spring seasons. The coupling methods CPL_mix and CPL_flx give similar biases of SST and other climate variables like T_2M, precipitation, PMSL, etc.

A possible reason for the cold SST bias of GCOAST-AHOI could be the underestimation of the downward shortwave radiation at the surface of ICON-CLM with the current model settings. A deeper analysis of the bias will be done in the next study, especially after re-running the simulations with the optimal settings of ICON-CLM, which will be found within the COPAT2 initiative of the CLM-Community. For example, the performance of ICON-CLM will be tuned by using the transient MACv2-SP aerosol data (Kinne, 2019) and modified namelist parameters related to cloud cover to improve the shortwave downward radiation and reduce the cold bias.

Despite the cold SST bias, ~~ICPL266~~ GCOAST-AHOI was able to capture the distribution of temperature, precipitation, mean sea level pressure and wind speed well, similar to the uncoupled ICON-CLM model. However, ~~-~~GCOAST-AHOI provides ~~a~~ larger biases in sea ice fraction ~~bias~~ and salinity ~~bias~~ over the Baltic Sea compared ~~with~~to the stand-alone ocean simulation (NEMO3.6) forced by ERA5 and ORAS5. The sea ice fraction bias is ~~linked~~link~~ed~~related to the cold T_2M bias in

ICPL266 and ICPL266_flx. Using the flux coupling method CPL_flx instead of CPL_mix doesn't strongly affect the bias of SST and climate variables but causes a larger sea ice fraction positive bias over the Baltic Sea. In the future study, a new simulation of ICPL266 with the CPL_var coupling method will be conducted and compared with the current ICPL266 and ICPL266_flx experiments to investigate the impact of the coupling methods on the sea ice simulation.

The salinity bias is attributed to the dry runoff ~~dry~~ bias of ICPL266 compared to the climatology, with the largest bias values are found near the Ems and Newa ~~river mouths.~~estuaries. The dry runoff bias near the Ems and Newa River mouths is due to a mismatch of the river mouth locations between the climatology and ~~the~~ ICPL266. An adjustment of the Newa River mouth location must be ~~done~~made to ~~let the~~allow the Newa ~~r~~River runoff ~~from Newa run~~to flow into the Gulf of Finland. ~~Effect of~~The ~~E~~effect of the river runoff~~and discharge~~ bias on salinity in the deeper layers of the ocean should be analyzed in the future ~~study~~.

In addition, ~~The~~ added value of the coupled model compared to the stand-alone model is usually found in the case of extreme events (Ho-Hagemann et al., 2015, 2017, 2020; Wiese et al., 2019, 2020). Therefore, we will analyze the model simulations with a focus on extreme events in the next study.

Our present study shows that the RESM GCOAST-AHOI can be a useful tool for conducting long-term regional climate simulations. The new OASIS3-MCT coupling interface OMCI implemented in the ICON-CLM model adds a possibility ~~makes the ICON-CLM model more flexible~~ to couple ICON-CLM with an external ocean model and an external hydrological discharge model, not only with NEMO and HD, using OASIS3-MCT instead of YAC. Given that the standalone model components for each the atmosphere and the ocean are available for a specific geographical domain, it is also quite easy to apply GCOAST-AHOI to other regions. Besides preparing the lateral boundary conditions for NEMO over the new domain, and the OASIS input files (as described in Supplementary S6~~5~~ and ~~S6~~S7), it is necessary to prepare several new parameter files so that OASIS3-MCT can exchange the discharge from HD to NEMO without interpolation. On the one hand, these are files for the general setup of the HD model. The creation of these files is described in Sect. 3 of the HD model readme mark down file included in the HD model package (Hagemann et al. 2023). On the other hand, this includes the HD model coupling file, which is used for coupling via OASIS. Instructions for its generation are provided in Section 2.1 of a markdown file dedicated to the HD model coupling exercises (Hagemann et al. 2023).

ICON-CLM with OMCI is also used to couple ICON-CLM with NEMO v4.2 over the GCOAST domain

(manuscript in preparation) and with NEMO-MED v3.6 over the Mediterranean Sea region in the CLM-Community. OMCI for the older ICON version 2.6.4 can be found in Ho-Hagemann (2022).

Recently, the ICON Consortium has developed and released the Community ~~interface~~ Interface (~~Comin~~ComIn) for the ICON model to allow ICON to be coupled with external model components. The main challenge for the external model component coupling is the initial splitting of MPI_COMM_WORLD, which is done in ICON by a grouping of the mpi communicators (MPI-handshake) (M. Hanke, pers. communication, 2024). There are about 40 ComIn entry points in the new release version of ICON. Using the ComIn entry points ~~will~~does not require any additional patching of the ICON source code. A coupling interface to an external model such as OMCI must be moved into a ComIn-plugin to connect to the entry points in the ICON source code. In addition, t~~.~~he communicator splitting using the MPI-handshake algorithm must be implemented in the NEMO and HD source code.~~In the future, OMCI will be integrated into tComin via a plugin. For example, instead of calling cpl_oas_init in the ICON source code, the start_mpi subroutine of ICON will call e.g. Comin_Init and within the Comin_Init subroutine, the cpl_oas_init will be called. It is similar for other subroutines of OMCI, i.e. they can be called in the Comin interface instead of directly in the main subroutines of ICON as it is currently done. In combination with the external coupler YAC, there will be an easier maintainable code for the coupling interface. Using the ComIn entry points will not require any additional patching of the ICON source code.~~

Currently, also a limited area mode of the ocean model (ICON-O-LAM) is being developed within the ICON consortium. This can be coupled with ICON-CLM via the YAC coupler in the ICON-Seamless framework. When that RESM will be available in the future and will be applied for the EURO-CORDEX domain, its simulation can be compared with the simulations of GCOAST-AHOI as a good reference. Investigating difference in simulations of the two RESMs could be helpful to understand better the coupling interactions and feedback between model components of the climate system.

Supplementary Materials: Supplementary material is available online together with the submitted manuscript. ~~Data and software used for the analyses in this study are available from the authors upon request.~~

Author Contributions: H.T.M. H.-H. developed the OMCI in ICON-CLM and HD, modified the OMCI in NEMO, designed the experiments and carried them out, analyzed the results; H.T.M. H.-H. prepared the manuscript with contributions from all co-authors; V.M. contributed to analyze the simulations; S.P contributed to develop the OMCI in ICON-CLM; I.F. supported debugging the GCOAST-AHOI on the DKRZ HPC system. All authors have read and agreed to the published version of the manuscript.

Funding: This study was conducted within the CoastalFutures project that was funded by the German Federal Ministry

of Education and Research under grant number 03F0911E. Moreover, it has been supported by funding from the German project REKLIM. The work described in this article has received funding from the Initiative and Networking Fund of the Helmholtz Association through the project "Advanced Earth System Modelling Capacity (ESM)". The content of the article is the sole responsibility of the author(s) and it does not represent the opinion of the Helmholtz Association, and the Helmholtz Association is not responsible for any use that might be made of the information contained. The study also contributes to the fourth programm-oriented funding phase (PoF IV) of the Helmholtz Association of German Research Centers.

Acknowledgements: The authors are grateful to the following entities: The German Climate Computing Center (DKRZ) provided the computer hardware for the Limited Area Modelling simulations in the project "Regional Atmospheric Modelling"; We acknowledge the E-OBS dataset from the EU-FP6 project UERRA (http://www.uerra.eu) and the Copernicus Climate Change Service, and the data providers in the ECA20ndD project (https://www.ecad.eu). We appreciate the use of the ERA5 reanalysis product that was provided by the European Centre for Medium-Range Weather Forecasts (ECMWF). ERA5 data reformatted by the CLM community provided via the DKRZ data pool were used. This study has been conducted using E.U. Copernicus Marine Service Information (https://doi.org/10.48670/moi-00165). We express our thanks to CERFACS (France) for the availability of the OASIS3-MCT coupler, especially to Eric Maisonnave for a support with the LUCIA tool in OASIS3-MCT. We thank Sebastian Grayek (formerly at Helmholtz-Zentrum Hereon) for preparing the NEMO lateral boundary conditions. We are also grateful Daniel Rieger and Daniel Reinert (DWD) for their advice on ICON source code. We thank Stefan Hagemann (Hereon) for proving the information on setting the HD model,~~.~~ and thank Beate Geyer (Hereon) for the information on NUKLEUS settings for the ICON-CLM model. We express our thanks to Panagiotis Adamidis (DKRZ) for the great technical support, and thanks to Moritz Hanke (DKRZ) for his comments and related information on YAC and ComIn in ICON.

Code and data availability: ICON is available to the community under a permissive open source licence (BSD-3C). One can download the newest released version at https://gitlab.dkrz.de/icon/icon-model. The source code of ICON v2.6.6 including the OMCI is published on Zenodo (https://doi.org/10.5281/zenodo.~~10877618~~11057794~~)~~). Note that ICON v2.6.6 was released before the open source release of ICON. As this version still comprises 3rd party modules with a more restrictive license, we had to change the file access from public to available upon request.

The NEMO source code is freely available and distributed under CeCILL license (GNU GPL compatible). To download the NEMO reference version (for now revision 3.6):

svn co http://forge.ipsl.jussieu.fr/nemo/svn/NEMO/releases/release-3.6/NEMOGCM

The modified NEMO v3.6 source code for different coupling methods are published on Zenodo (https://doi.org/10.5281/zenodo.~~10877618~~11057794~~)~~).

The HD source code is available at https://doi.org/10.5281/zenodo.4893099.

Source code of OASIS3-MCT v4.0 with small modifications in lib/psmile/src/GPTLget_memusage.c and lib/mct/mct/m_AttrVectComms.F90 is published on Zenodo (https://doi.org/10.5281/zenodo.11057794).

Input data, run-scripts, evaluation scripts are published on Zenodo (https://doi.org/10.5281/zenodo.11057794). Because of its huge volume, forcing data used for this study is available from the authors upon request.

Conflicts of Interest: The authors declare no conflict of interest. The funders had no role in the design of the study; in the collection, analyses, or interpretation of data; in the writing of the manuscript, or in the decision to publish the

results.

References

Bauer, T. P., Holtermann, P., Heinold, B., Radtke, H., Knoth, O., and Klingbeil, K.: ICONGETM v1.0 – flexible NUOPC driven two-way coupling via ESMF exchange grids between the unstructured-grid atmosphere model ICON and the structured grid coastal ocean model GETM, Geosci. Model Dev., 14, 4843–4863, https://doi.org/10.5194/gmd-14-4843-2021, 2021.

Bechtold, P., Kohler, M., Jung, T., Leutbecher, M., Rodwell, M., Vitart, F., and Balsamo, G.: Advances in predicting atmospheric variability with the ECMWF model, 2008: From synoptic to decadal time-scales. Quart. J. Roy. Meteor. Soc., 134, 1337–1351, https://doi.org/10.1002/qj.289, 2008.

Copernicus Climate Change Service, Climate Data Store: ORAS5 global ocean reanalysis monthly data from 1958 to present, Copernicus Climate Change Service (C3S) Climate Data Store (CDS), https://doi.org/10.24381/cds.67e8eeb7, 2021.

Daewel, U., and Schrum, C.: Simulating long-term dynamics of the coupled North Sea and Baltic Sea ecosystem with ECOSMO II: Model description and validation. J. Marine Syst. 119–120, 30–49, 2013.

Dipankar, A., Stevens, B., Heinze, R., Moseley, C., Zängl, G., Giorgetta, M., and Brdar, S.: Large eddy simulation using the general circulation model ICON, J. Adv. Model. Earth Syst., 7, 963–986, doi:10.1002/2015MS000431, 2015.

Doms, G., and Coauthors: A description of the nonhydrostatic regional model LM. Part II: Physical parameterization. Tech. Rep., Deutscher Wetterdienst, Offenbach, Germany, 146 pp., http://www.cosmo-model.org/content/model/documentation/core/cosmoPhysParamtr.pdf, 2004.

Farkas, C., and Skarbøvik, E.: OSPAR Contracting Parties' RID 2019 Data Report, NIBIO – Norwegian Institute for Bioeconomy Research, 57 pp., 2021.

Giorgetta, M. A., Brokopf, R., Crueger, T., Esch, M., Fiedler, S., Helmert, J., et al.: ICON-A, the atmosphere component of the ICON EarthSystem Model: I. Model description. Journal of Advances in Modeling Earth Systems. https://doi.org/10.1002/2017MS001242, 2018.

Good, S., Fiedler, E., Mao, C., Martin, M.J., Maycock, A., Reid, R., Roberts-Jones, J., Searle, T., Waters, J., While, J., and Worsfold, M.: The Current Configuration of the OSTIA System for Operational Production of Foundation Sea Surface Temperature and Ice Concentration Analyses. Remote Sens., 12, 720, https://doi.org/10.3390/rs12040720, 2020.

Hagemann, S., and Dümenil, L.: A parametrization of the lateral waterflow for the global scale, Climate Dyn., 14, 17–31, https://doi.org/10.1007/s003820050205, 1998.

Hagemann, S., and Ho-Hagemann, H.T.M.: The Hydrological Discharge Model - a river runoff component for offline and coupled model applications (5.0.0), Zenodo. https://doi.org/10.5281/zenodo.4893099, 2021.

Hagemann, S., Stacke, T., and Ho-Hagemann, H.T.M.: High resolution discharge simulations over Europe and the Baltic Sea catchment, Frontiers in Earth Science, 8, https://doi.org/10.3389/feart.2020.00012, 2020.

Hagemann, S., Stacke, T.: Complementing ERA5 and E-OBS with high-resolution river discharge over Europe. Oceanologia 65: 230-248, doi:10.1016/j.oceano.2022.07.003, 2022.

Hagemann, S., Ho-Hagemann, H. T. M., and Hanke, M.: The Hydrological Discharge Model - a river runoff component for offline and coupled model applications (5.2.2), Zenodo, https://doi.org/10.5281/zenodo.10405875, 2023.

Hagemann, S., Nguyen, T. T., and Ho-Hagemann, H. T. M.: A three-part bias correction of simulated European river runoff to force ocean models, EGUsphere [preprint], https://doi.org/10.5194/egusphere-2024-1774, 2024.

Hanke, M., Redler, R., Holfeld, T., and Yastremsky, M.: YAC 1.2.0: new aspects for coupling software in Earth system modelling, Geosci. Model Dev., 9, 2755-2769, https://doi.org/10.5194/gmd-9-2755-201, 2016.

Haylock, M., Hofstra, N., Klein Tank, A., Klok, E., Jones, P., and New, M.: A European daily high-resolution gridded data set of surface temperature and precipitation for 1950–2006, J. Geophys. Res.-Atmos., 113, D20119, https://doi.org/10.1029/2008JD010201, 2008.

Heinze, R., Dipankar, A., Henken, C. C., Moseley, C., Sourdeval, O., Trömel, S., Xie, X., Adamidis, P., Ament, F., Baars, H., Barthlott, C., Behrendt, A., Blahak, U., Bley, S., Brdar, S., Brueck, M., Crewell, S., Deneke,H., Di Girolamo,P., Evaristo, R., Fischer, J., Frank, C., Friederichs, P., Göcke, T., Gorges, K., Hande, L., Hanke, M.,

Hansen, A., Hege, H-C., Hoose, C., Jahns, T., Kalthoff, N., Klocke, D., Kneifel, S., Knippertz, P., Kuhn, A., van Laar, T., Macke, A., Maurer, V., Mayer, B., Meyer, C. I., Muppa, S. K., Neggers, R. A. J., Orlandi, E., Pantillon, F., Pospichal, B., Röber,N., Scheck, L., Seifert, A., Seifert, P., Senf, F., Siligam, P., Simmer, C., Steinke, S., Stevens, B., Wapler, K., Weniger, M.,Wulfmeyer, V., Zängl, G., Zhang, D., and Quaas, J.: Large-eddy simulations over Germany using ICON: A comprehensive evaluation, Q. J. Roy. Meteor. Soc., 143, 69–100, 2017.

Hersbach, H., Bell, B., Berrisford, P., Hirahara, S., Horányi, A., Muñoz Sabater, J., et al.: The ERA5 global reanalysis, Q. J. Roy. Meteor. Soc., 146(730), 1999-2049. https://doi.org/10.1002/qj.3803, 2020.

Hill, C., DeLuca, C., Balaji, Suarez, M., and Da Silva, A.: The architecture of the Earth System Modeling Framework, Computing in Science Engineering, 6, 18–28, https://doi.org/10.1109/MCISE.2004.1255817, 2004.

Hogan, R. J., and Bozzo, A.: A flexible and efficient radiation scheme for the ECMWF model. J. Adv. Model Earth Sys., 10(8), 1990–2008, 2018.

Ho-Hagemann, H. T. M.: The OASIS3-MCT Coupling Interface for ICON-CLM (1.0.0). Zenodo. https://doi.org/10.5281/zenodo.5833118, 2022.

Ho-Hagemann, H. T. M.: Regional Earth system model GCOAST-AHOI v2.0 with ICON-CLM~~.~~ (1.0.1). Zenodo. https://doi.org/10.5281/zenodo.~~10877618~~11057794, 2024.

Ho-Hagemann, H. T. M., Hagemann, S., and Rockel, B.: On the role of soil moisture in the generation of heavy rainfall during the Oder flood event in July 1997, Tellus A 2015, 67, 28661, https://doi.org/10.3402/tellusa.v67.28661, 2015.

Ho-Hagemann, H. T. M., Gröger, M., Rockel, B., Zahn, M., Geyer, B., and Meier, H. E. M.: Effects of air-sea coupling over the North Sea and the Baltic Sea on simulated summer precipitation over Central Europe, Clim Dyn 49, 3851-3876. https://doi.org/10.1007/s00382-017-3546-8, 2017.

Ho-Hagemann, H. T. M., Hagemann, S., Grayek, S., Petrik, R., Rockel, B., Staneva, J., Feser, F., and Schrum, C.: Internal model variability of the regional coupled system model GCOAST-AHOI, Atmosphere, 11(3), 227. https://doi.org/10.3390/atmos11030227, 2020.

Jungclaus, J. H., Lorenz, S. J., Schmidt, H., Brovkin, V., Brüggemann, N., Chegini, F., et al.: The ICON Earth System Model version 1.0. Journal of Advances in Modeling Earth Systems, 14, e2021MS002813. https://doi.org/10.1029/2021MS002813, 2022.

Kinne, S.: Aerosol radiative effects with MACv2, Atmos. Chem. Phys., 19, 10919–10959, https://doi.org/10.5194/acp-19-10919-2019, 2019.

Korn, P.: Formulation of an unstructured grid model for global ocean dynamics. Journal of Computational Physics, 339, 525–552. https://doi.org/10.1016/j.jcp.2017.03.009, 2017.

Large, W. G., and S. Yeager: Diurnal to decadal global forcing for ocean and sea-ice models: the data sets and flux climatologies, NCAR Technical Note, NCAR/TN-460+STR, CGD Division of the National Center for Atmospheric Research, 2004.

Lewis, H.W., Castillo Sanchez, J.M., Siddorn, J., King, R.R., Tonani, M., Saulter, A., Sykes, P., Pequignet, A.-C., Weedon, G.P., Palmer, T., Staneva, J., and Bricheno, L.: Can wave coupling improve operational regional ocean forecasts for the north-west European Shelf?, Ocean Sci., 15, 669-690, https://doi.org/10.5194/os-15-669-2019, 2019.

Lemmen, C., Hofmeister, R., Klingbeil, K., Nasermoaddeli, M.H., Kerimoglu, O., Burchard, H., Kösters, F., and Wirtz, K.W.: Modular System for Shelves and Coasts (MOSSCO v1.0) – a flexible and multi-component framework for coupled coastal ocean ecosystem modelling, Geosci. Model Dev., 11, 915-935, https://doi.org/10.5194/gmd-11-915-2018, 2018.

Madec, G., Bourdallé-Badie, R., Bouttier, P.-A., Bricaud, C., Bruciaferri, D., Calvert, D., Chanut, J., Clementi, E., Coward, A., Delrosso, D., Ethé, C., Flavoni, S., Graham, T., Harle, J., Iovino, D., Lea, D., Lévy, C., Lovato, T., Martin, N., Masson, S., Mocavero, S., Paul, J., Rousset, C., Storkey, D., Storto, A., and Vancoppenolle, M.: NEMO ocean engine (Version v3.6-patch), Tech. rep., Pôle De Modélisation De L'institut Pierre-simon Laplace (IPSL), Zenodo, https://doi.org/10.5281/ZENODO.3248739, 2017.

Maisonnave E., and Caubel A.: LUCIA, load balancing tool for OASIS coupled systems, https://cerfacs.fr/wp-content/uploads/2018/10/GLOBC_TR_Maisonnave_lucia_arnaud_2014.pdf, 2014.

Pein, J., Eisele, A., Hofmeister, R., Sanders, T., Daewel, U., Stanev, E.V., van Beusekom, J., Staneva, J., and Schrum, C.: Nitrogen cycling in the Elbe estuary from a joint 3D-modelling and observational perspective, Biogeosciences Discuss., (July), 1–34, https://doi.org/10.5194/bg-2019-265, 2019.

Pfeifroth, U., Kothe, S., Müller, R., Trentmann, J., Hollmann, R., Fuchs, P., and Werscheck, M.: Surface Radiation Data Set – Heliosat (SARAH) – Edition 2, Satellite Application Facility on Climate Monitoring, https://doi.org/10.5676/EUM_SAF_CM/SARAH/V002, 2017.

Pham, T. V., Steger, C., Rockel, B., Keuler, K., Kirchner, I., Mertens, M., Rieger, D., Zängl, G., and Früh, B.: ICON in Climate Limited-area Mode (ICON release version 2.6.1): a new regional climate model, Geosci. Model Dev., 14, 985–1005, https://doi.org/10.5194/gmd-14-985-2021, 2021.

Raupach, M.R., and Shaw, R.H.: Averaging procedures for flow within vegetation canopies. Boundary-Layer Meteorol 22, 79–90. https://doi.org/10.1007/BF00128057, 1982.

Raschendorfer, M.: The new turbulence parameterization of LM. In: G. Doms and U. Schättler (Edts.): COSMO Newsletter No. 1, 89-97 (available at www.cosmo-model.org), 2001.

Reick, C., V. Gayler, D. Goll, and S. Hagemann et al.: JSBACH 3 - The land component of the MPI Earth System Model: Documentation of version 3.2, Berichte zur Erdsystemforschung, 240, Max Planck Institute for Meteorology, Hamburg, http://doi.org/10.17617/2.3279802, 2021.

Renault, L., Masson, S., Oerder, V., Colas, F., and McWilliams, J.C.: Modulation of the oceanic mesoscale activity by the mesoscale thermal feedback to the atmosphere, J. Phys. Oceanogr., 53, pp. 1651-1667, 10.1175/JPO-D-22-0256.1, 2023.

Rieger, D., Köhler, M., Hogan, R., Schäfer, S., Seifert, A., Lozar, A. D., and Zängl, G.: ecRad in ICON – Implementation Overview, Reports on ICON, Deutscher Wetterdienst, Offenbach, Germany, https://doi.org/10.5676/DWDpub/nwv/icon004, 2019.

Rockel, B., and Geyer, B.: SPICE (Starter Package for ICON-CLM Experiments) (2.1), Zenodo. https://doi.org/10.5281/zenodo.7298390, 2022.

Rockel, B., Will, A., and Hense, A.: The regional climate model COSMO-CLM (CCLM), Meteorol. Z. 2008, 17, 347–348. doi:10.1127/0941-2948/2008/0309, 2008.

Russo, E., Geyer, B., Petrik, P., Keuler, K., Adinol, M., Feldmann, H., Goergen, K., Kerkweg, A., Khain, P., Ludwig, P., Mertens, M., Pothapakula, P., Raffa, M., Rockel, B., Schulz, J.-P., Sulis, M., Ho-Hagemann, H. T. M., Truhetz, H., Uzan, L., Voggenberger, U., and Steger, C.: CLM Community WG EVAL, COordinated Parameter Testing project 2 (COPAT2): COSMO-CLM 6.0 clm1 recommended model configuration, COSMO Technical Reports, No. 51, https://doi.org/10.5676/DWD_pub/nwv/cosmo-tr_51, 2024.

Schloen, J., Stanev, E.V., and Grashorn, S.: Wave-current interactions in the southern North Sea: The impact on salinity. Ocean Modelling 111 (2017) 19–37, https://doi.org/10.1016/j.ocemod.2017.01.003, 2017.

Schrodin, R., and Heise, E.: The multi-layer-version of the DWD soil model TERRA/LM. Consortium for Small-Scale Modelling (COSMO) Tech. Rep., 2, 16, 2001.

Shrestha, P., Sulis, M., Masbou, M., Kollet, S., and Simmer, C.: A scale-consistent terrestrial systems modeling platform based on COSMO, CLM, and ParFlow, Mon. Weather Rev., 142, 3466–3483, 2014.

Schrodin, R., and Heise, E.: The multi-layer-version of the DWD soil model TERRA/LM. Consortium for Small-Scale Modelling (COSMO) Tech. Rep 2001, 2, 16, 2001.

Schulz, J.-P., Vogel, G., Becker, C., Kothe, S., Rummel, U., Ahrens, B.: Evaluation of the ground heat flux simulated by a multi-layer land surface scheme using high-quality observations at grass land and bare soil Meteorol. Z., 25, pp. 607-620, https://doi.org/10.1127/metz/2016/0537, 2016.

Schulz, J.-P., and Vogel, G.: Improving the processes in the land surface scheme TERRA: bare soil evaporation and skin temperature Atmosphere, 11, p. 513, https://doi.org/10.3390/atmos11050513, 2020.

Slavik, K., Lemmen, C., Zhang, W., Kerimoglu, O., Klingbeil, K., and Wirtz, K.W. The large scale impact of offshore windfarm structures on pelagic primary production in the southern North Sea, Hydrobiologia (2019) 845: 35, https://doi.org/10.1007/s10750-018-3653-5, 2019.

Staneva, J., Alari, V., Breivik, Ø., Bidlot, J.-R., and Mogensen, K.: Effects of wave-induced forcing on a circulation model of the North Sea, Ocean Dynamics, https://doi.org/10.1007/s10236-016-1009-0, 2016.

Staneva, J., Schrum, C., Behrens, A., Grayek, S., Ho-Hagemann, H., Alari, V., Breivik, Ø., and Bidlot, J.-R.: A North Sea - Baltic Sea regional coupled models: atmosphere, wind, waves and ocean. In: Buch, E., Fernández, V., Eparkhina, D., Gorringe, P., and Nolan, G. (Eds.): Operational Oceanography serving Sustainable Marine Development, Proceedings of the Eight EuroGOOS International Conference, 516 pp, ISBN 978-2-9601883-3-2, 2018.

Stevens, B., Fiedler, S., Kinne, S., Peters, K., Rast, S., Müsse, J., Smith, S. J., and Mauritsen, T.: MACv2-SP: a parameterization of anthropogenic aerosol optical properties and an associated Twomey effect for use in CMIP6, Geosci. Model Dev., 10, 433–452, https://doi.org/10.5194/gmd-10-433-2017, 2017.

Svendsen, L. M., and Gustafsson, B.: Waterborne nitrogen and phosphorus inputs and water flow to the Baltic Sea 1995-2018. https://helcom.fi/baltic-sea-trends/environment-fact-sheets/eutrophication/, 2022.

Tegen, I., P. Hollrigl, M. Chin, I. Fung, D. Jacob, and Penner, J.: Contribution of different aerosol species to the global aerosol extinction optical thickness: Estimates from model results, J. Geophys. Res., 102, 23895-23915, 1997.

Tiedtke, M. A comprehensive mass flux scheme for cumulus parameterization in large-scale models. Mon. Weather Rev. 1989, 117, 1779–1800.

Valcke, S., Craig, T., and Coquart, L.: OASIS3-MCT user guide, OASIS3-MCT 3.0. Technical Report TR/CMGC/15/38, CERFACS, Toulouse, France, CERFACS/CNRS SUC URA No 1875, 2015.

Van den Besselaar, E., Haylock, M., Van der Schrier, G., and Klein Tank, A.: A European daily high-resolution observational gridded data set of sea level pressure, J. Geophys. Res.-Atmos., 116, D11110, https://doi.org/10.1029/2010JD015468, 2011.

Wahle, K., Staneva, J., Koch, W., Fenoglio-Marc, L., Ho-Hagemann, H.T.M., and Stanev, E.V.: An atmosphere–wave regional coupled model: improving predictions of wave heights and surface winds in the southern North Sea, Ocean Sci., 13, 289-301, https://doi.org/10.5194/os-13-289-2017, 2017.

Wiese, A., Staneva, J., Ho-Hagemann, H. T. M., Grayek, S., Koch, W., and Schrum, C.: Internal Model Variability of Ensemble Simulations with a Regional Coupled Wave-Atmosphere Model GCOAST, Frontiers in Marine Science, 7, 596843, https://doi.org/10.3389/fmars.2020.596843, 2020.

Wiese, A., Stanev, E., Koch, W., Behrens, A., Geyer, B., and Staneva, J.: The Impact of the Two-Way Coupling between Wind Wave and Atmospheric Models on the Lower Atmosphere over the North Sea, Atmosphere 2019, 10, 386, https://doi.org/10.3390/atmos10070386, 2019.

Will, A., Akhtar, N., Brauch, J., Breil, M., Davin, E., Ho-Hagemann, H.T.M., Maisonnave, E., Thürkow, M., and Weiher, S.: The COSMO-CLM 4.8 regional climate model coupled to regional ocean, land surface and global earth system models using OASIS3-MCT: Description and performance, Geosci. Model Dev. 2017, 10, 1549–1586. doi:10.5194/gmd-10-1549-2017, 2017.

Zängl, G., Reinert, D., Rípodas, P., and Baldauf, M.: The ICON (ICOsahedral Non-hydrostatic) modelling framework of DWD and MPI-M: Description of the non-hydrostatic dynamical core, Q. J. Roy. Meteor. Soc., 141, 563–579, https://doi.org/10.1002/qj.2378, 2015.

Zhang, Y. and Perrie, W.: Feedback Mechanisms For The Atmosphere And Ocean Surface, Boundary-Layer Meteorology 100, 321–348. https://doi.org/10.1023/A:1018996505248, 2001.

Zhang, W., Wirtz, K., Daewel, U., Wrede, A., Kröncke, I., Kuhn, G., Neumann, A., Meyer, J., Ma, M., and Schrum, C.: The budget of macrobenthic reworked organic carbon - a modelling case study of the North Sea, Journal of Geophysical Research-Biogeosciences, https://doi.org/10.1029/2019JG005109, 2019.

Table 1: Model configuration

Configuration	ICON	NEMO	HD	Coupler OASIS3-MCT
Version	v2.6.6	v3.6	v5.1	v4.0
Domain	EURO-CORDEX	North Sea, Baltic Sea, North Atlantic	Europe	-
Resolution	~ 12 km	~ 3.7 km	~ 8 km	-
Grid points	231660	902 x 777	960 x 540	
Time step	100 s	90 s	3600 s	3600 s
Forcing	ERA5	ORAS5, OTIS	-	-

Table 2: Model experiments

Experiment	Description
ICON266	Uncoupled ICON-CLM v2.6.6 forced by ERA5
ICPL266	Coupled GCOAST-AHOI forced by ERA5 and ORAS5
ICPL266_noNewa	Coupled GCOAST-AHOI forced by ERA5 and ORAS5, Newa ~~river~~ River mouth is located on the buffer zone of NEMO grid.
ICPL266_flx	Coupled GCOAST-AHOI forced by ERA5 and ORAS5, coupling method CPL_flx
NEMO3.6	Stand-alone NEMO v3.6 forced by ERA5 and ORAS5
HDICON266	Stand-alone HD v5.1 forced by surface runoff and sub-surface runoff of ICON266

~~*Table 3: Number of requested nodes/processors for performance tests of GCOAST-AHOI on Levante. NPX and NPY are the processors for NEMO corresponding to x and y dimensions, respectively.*~~

~~Case~~	~~Nodes~~	~~Total processors~~	~~Processors for ICON~~	~~Processors for NEMO~~	~~Processors for HD~~
~~A~~	~~25~~	~~3200~~	~~1599~~	~~NPX x NPY = 40 x 40 = 1600~~	~~1~~
~~B~~	~~30~~	~~3840~~	~~2239~~	~~NPX x NPY = 40 x 40 = 1600~~	~~1~~
~~C~~	~~30~~	~~3840~~	~~1839~~	~~NPX x NPY = 50 x 40 = 2000~~	~~1~~
~~D~~	~~40~~	~~5120~~	~~3519~~	~~NPX x NPY = 40 x 40 = 1600~~	~~1~~
~~E~~	~~40~~	~~5120~~	~~2719~~	~~NPX x NPY = 60 x 40 = 2400~~	~~1~~

Table 34: Seasonal discharge (m^3/s) of ICPL266 and HDICON266 summed over the North Sea, the Baltic Sea during the period of 2010-2018. Diff. (%) is the difference of ICPL266 to HDICON266.

Areas	North Sea			Baltic Sea		
Seasons	**ICPL266**	**HDICON266**	**Diff. (%)**	**ICPL266**	**HDICON266**	**Diff. (%)**
DJF	7356	7687	-3.31	9148	10864	-15.80
MAM	6896	7438	-5.42	18788	19884	-5.51
JJA	5103	5482	-3.79	9837	10990	-10.49
SON	4352	4857	-5.05	6755	8056	-16.15
ANN	5927	6366	-4.39	11132	12449	-10.58

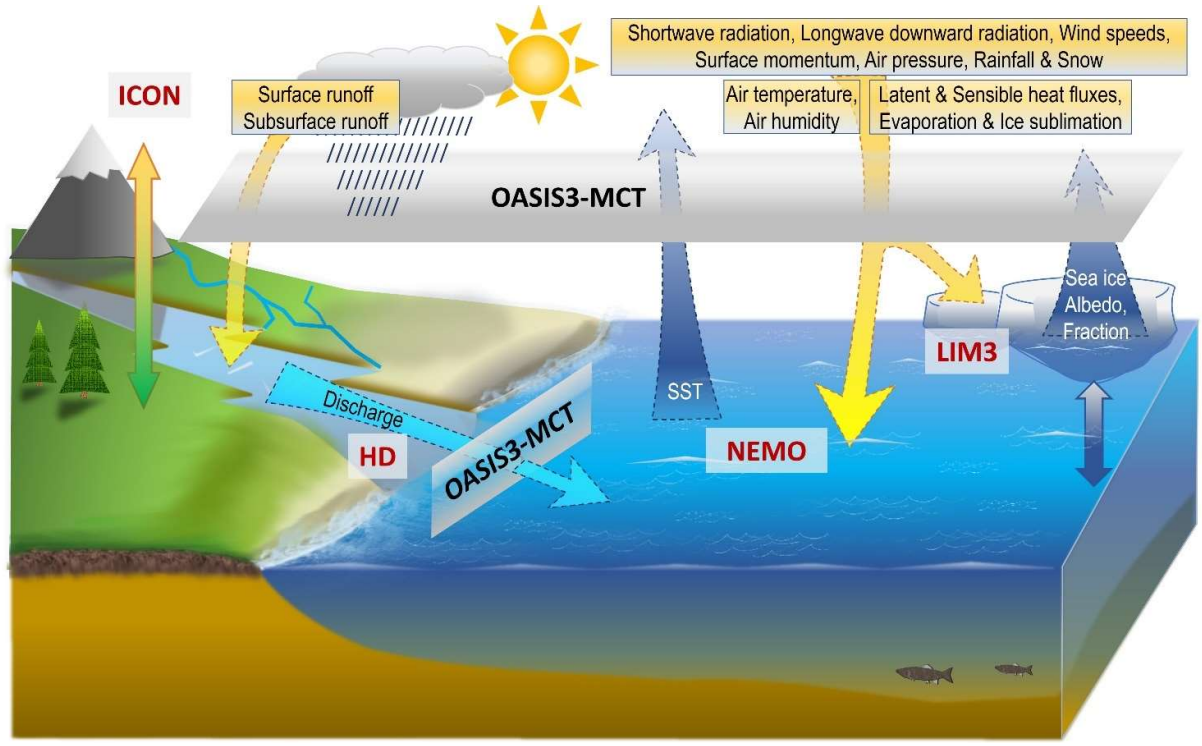

823

Figure 1: Model components of GCOAST-AHOI and variables exchanged via the OASIS3-MCT coupler. Two solid arrows display the communication between atmosphere-land (yellow-green arrow) and ocean-sea ice (gray-blue arrow), which is done via subroutines inside ICON-CLM and NEMO, respectively. Dotted arrows show the transfer between components via the OASIS interface. Yellow arrows present atmospheric transfer to ocean-sea ice and river runoff. The cyan arrow shows the discharge from the river to the ocean. Blue arrows demonstrate the transfer of sea surface temperature (SST) from the ocean as well as the sea ice albedo and sea ice fraction to the atmosphere.

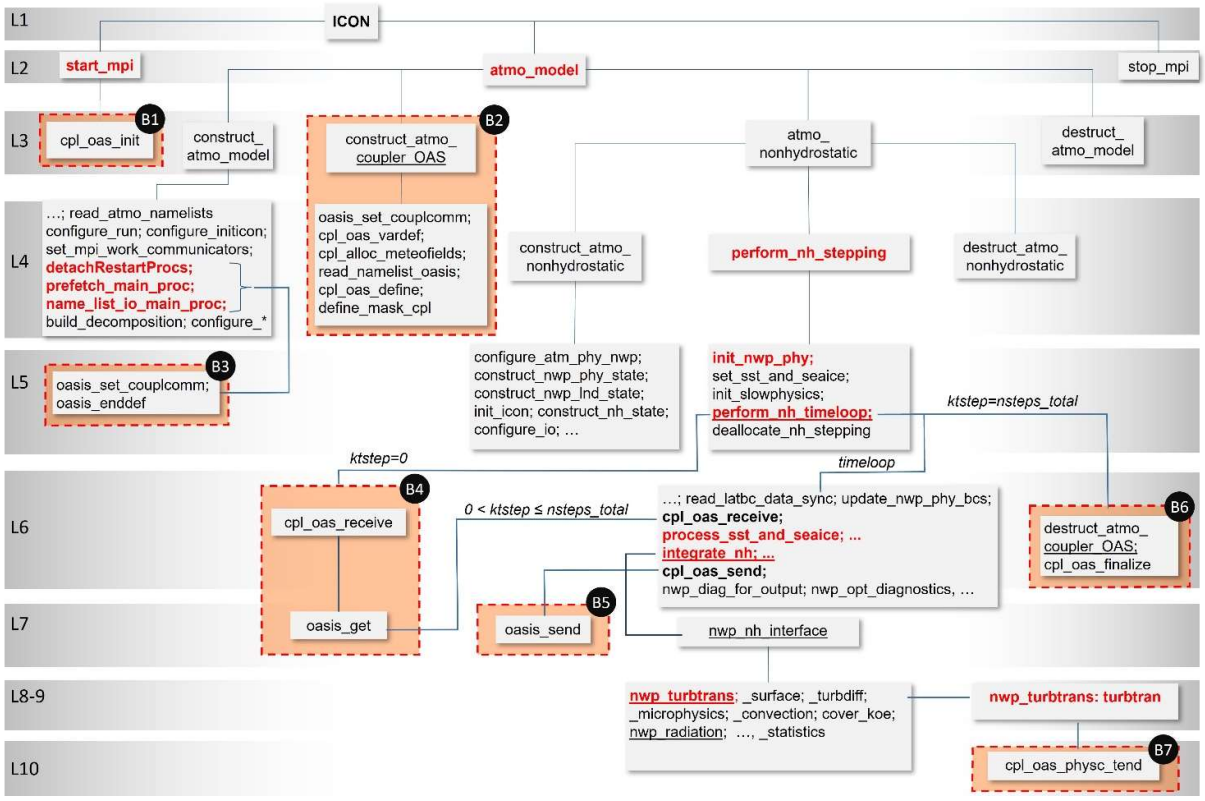

824

Figure 2: Flowchart of ICON-NWP/ICON-CLM with the OASIS3-MCT coupling interface OMCI. The running sequence is from top to bottom, and from left to right. "L1" indicates the Level 1 – main program ICON, etc. At the levels 2 to 6, 8 and 9, subroutines (in red text) of ICON are modified by the coupling. At the levels 3 to 7 and 10, subroutines added for OMCI are shown in orange boxes (B1-B7).

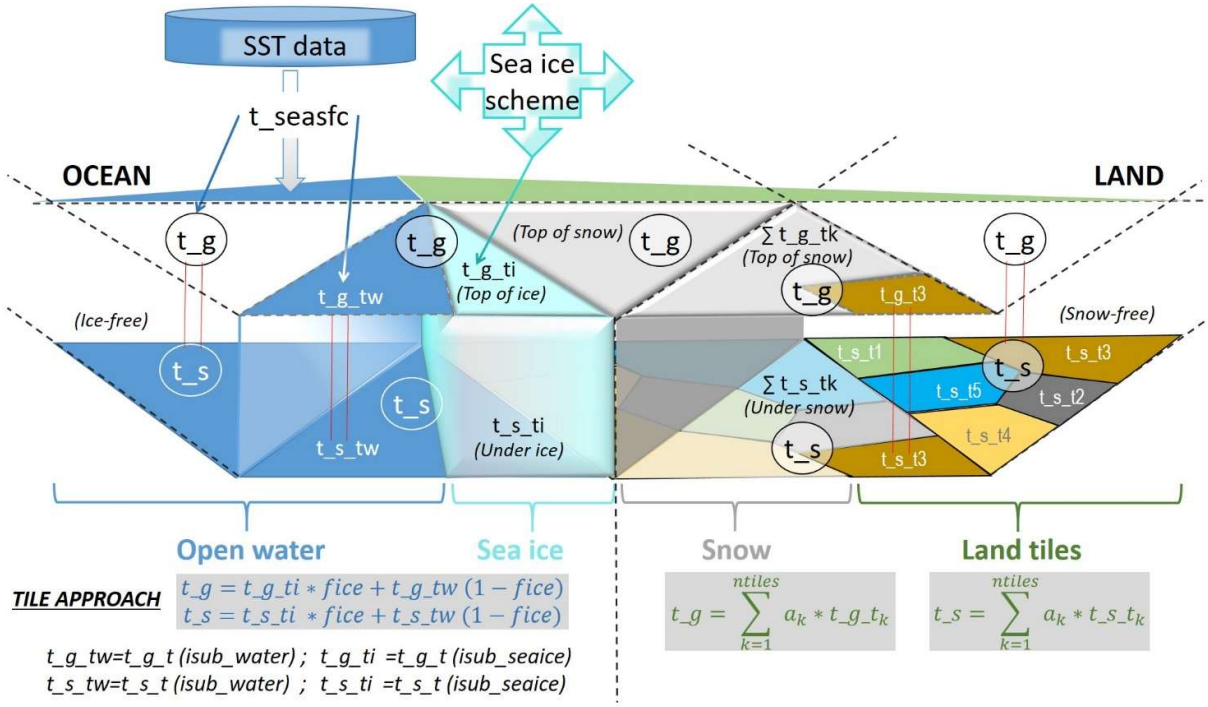

825

Figure 3: Surface temperature exchange between atmosphere and ocean/land in ICON and GCOAST-AHOI.

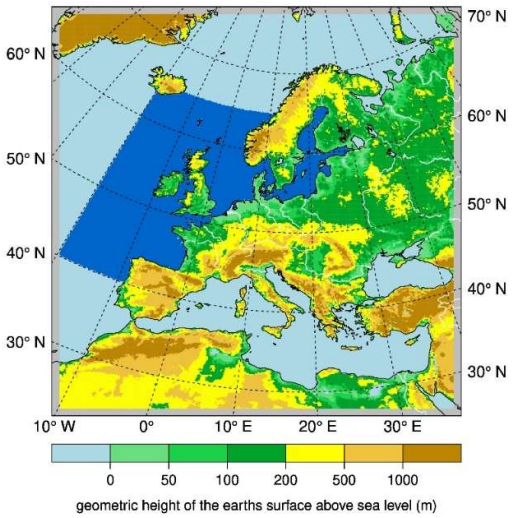

826

Figure 4: Integration domains of ICON and HD (EURO-CORDEX) and of NEMO-LIM3 (dark blue).

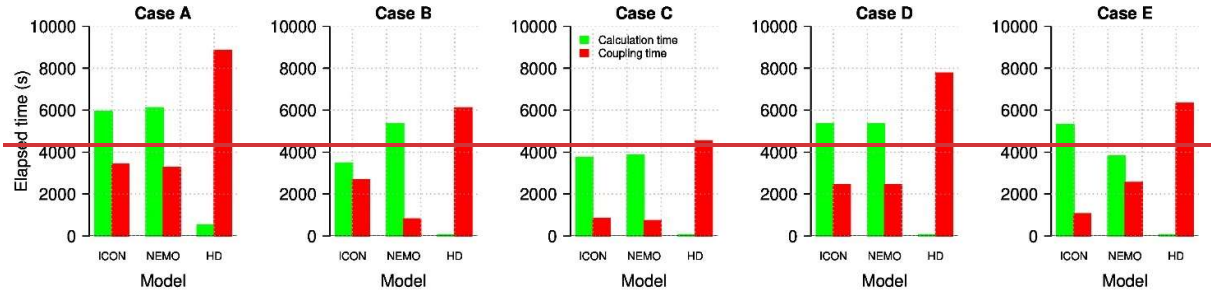

827

~~*Figure 5: Calculation time (green) versus coupling exchange duration including time spent to wait for other model components (red). See table 3 for a detailed view of the node balance of the displayed cases.*~~

828

a) ICPL266

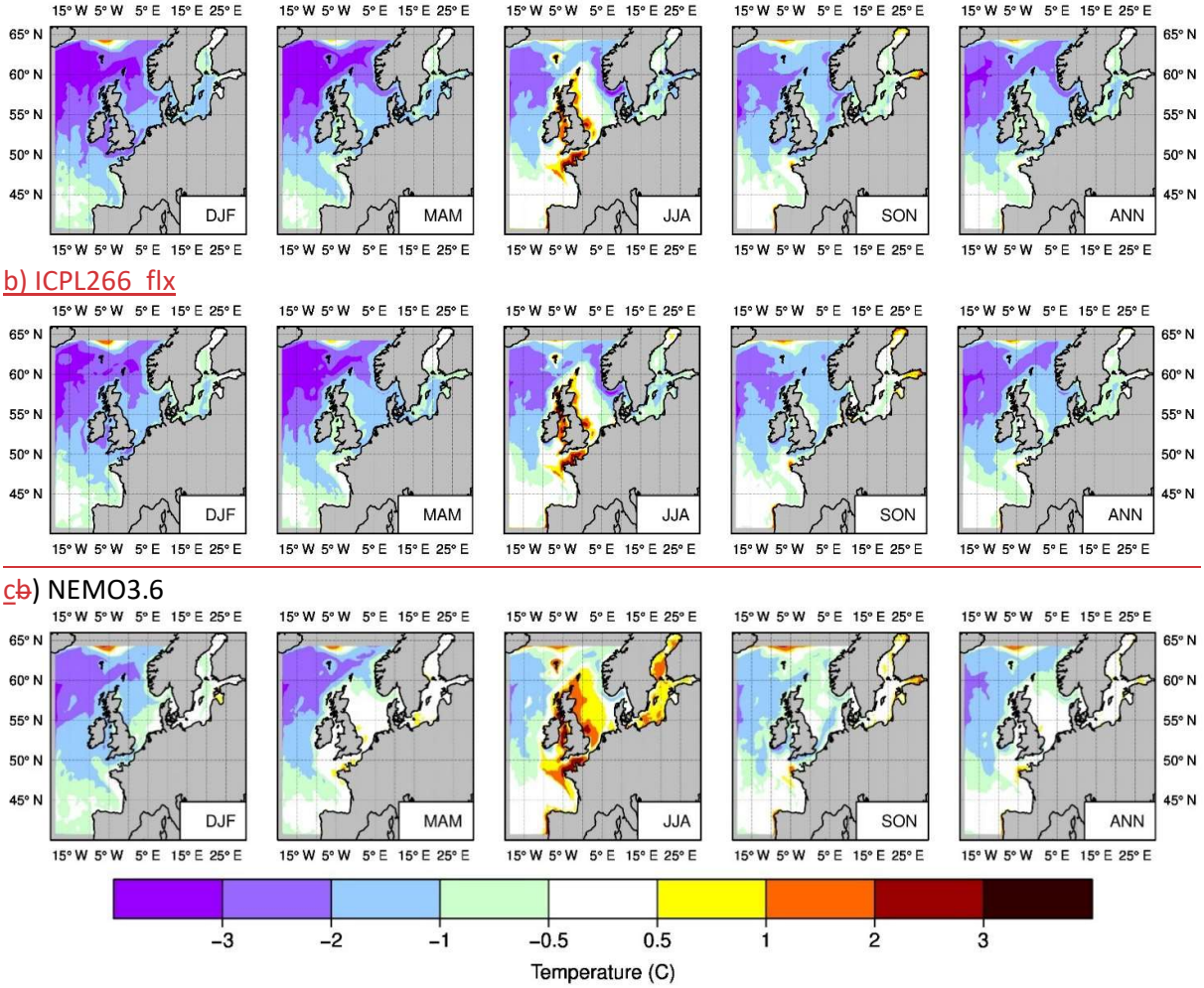

Figure 5: Seasonal (DJF, MAM, JJA, SON) and annual (ANN) mean of sea surface temperature (K) bias of a) ICPL266, b) ICPL266_flx and c) NEMO3.6 with respect to the OSTIA data for the period of 2010-2018 over the GCOAST domain.

a) ICON266

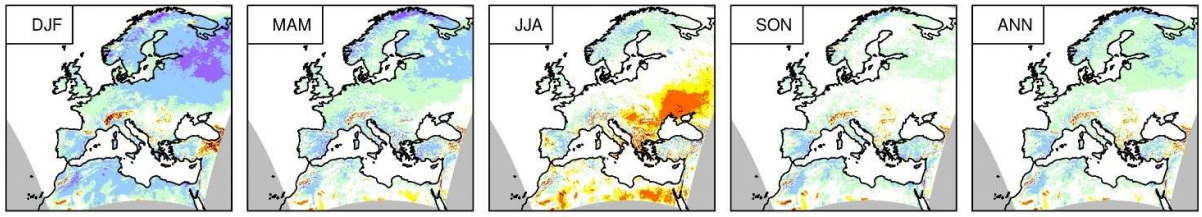

b) ICPL266

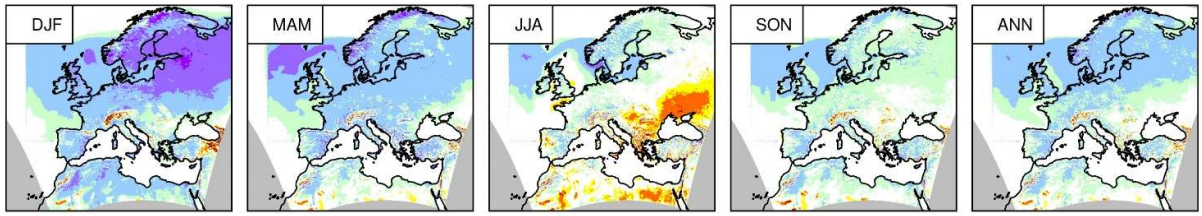

c) ICPL266_flx

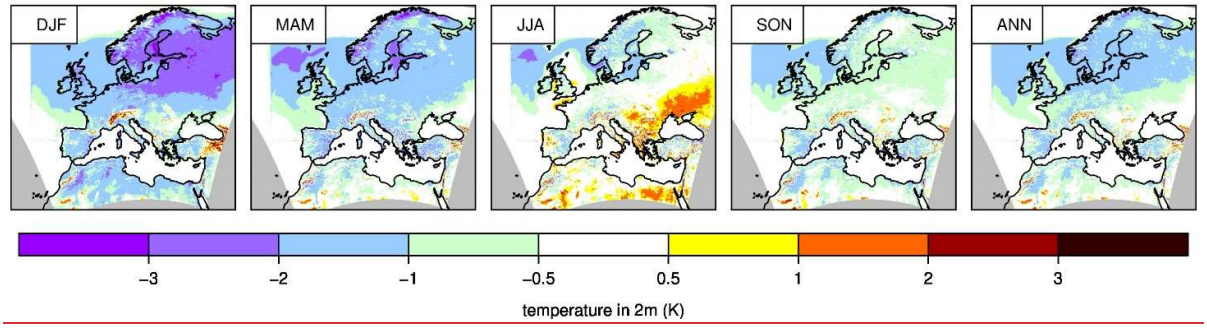

Figure ~~7~~6: Seasonal (DJF, MAM, JJA, SON) and annual (ANN) mean of 2m air temperature (K) difference ~~between~~ of a) ICON266, ~~and~~ b) ICPL266 and c) ICPL266_flx ~~compared~~ to the ERA5 reanalysis data for the period of 2010-2018.

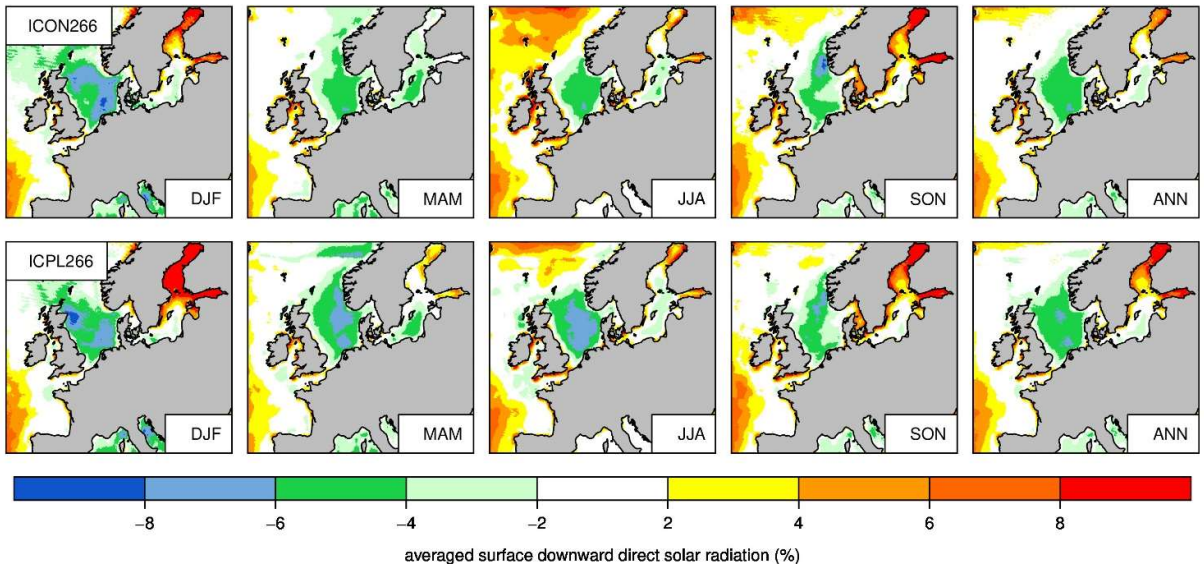

Figure ~~7~~8: Seasonal (DJF, MAM, JJA, SON) and annual (ANN) mean of shortwave downward radiation bias (%) of ICON266 (top) and ICPL266 (bottom) compared to the ERA5 data for the period of 2010-2018 over the GCOAST domain.

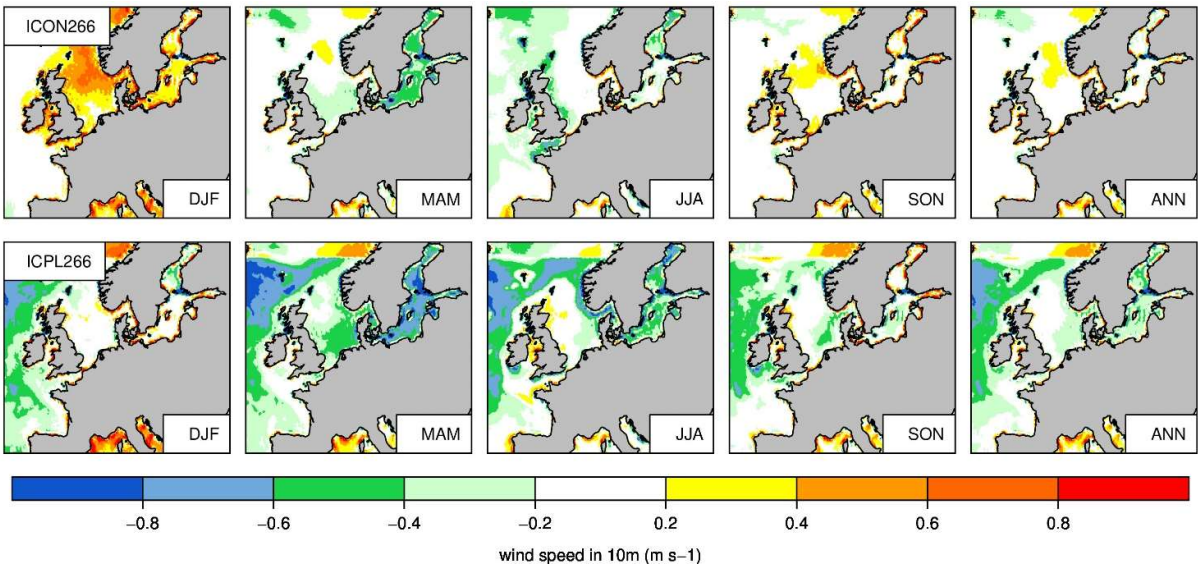

Figure ~~89~~: Seasonal (DJF, MAM, JJA, SON) and annual (ANN) mean 10-M wind speed bias (m s $^{-1}$) of ICON266 (top) and ICPL266 (bottom) compared to the ERA5 data for the period of 2010-2018 over the GCOAST domain.

a) ICON266

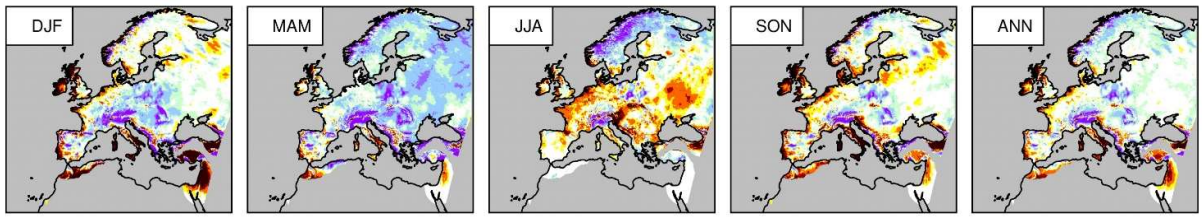

b) ICPL266

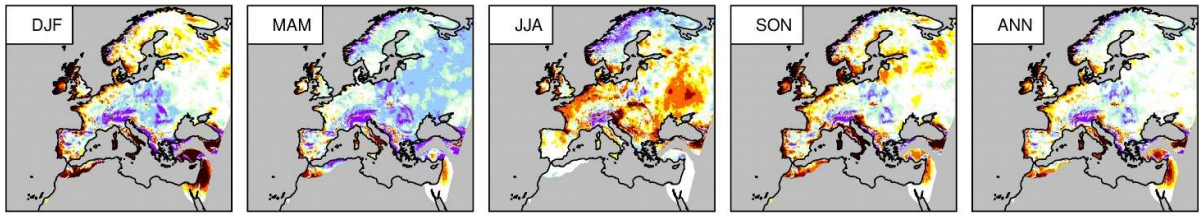

c) ICPL266_flx

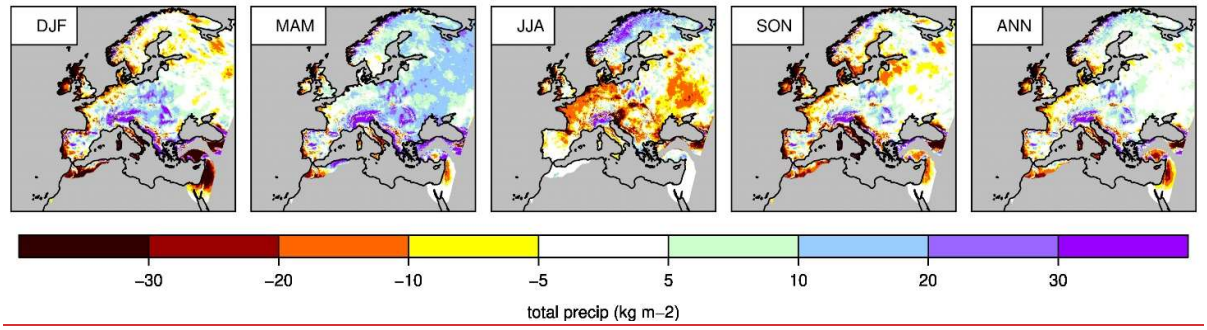

Figure 9~~10~~: Seasonal (DJF, MAM, JJA, SON) and annual (ANN) difference of precipitation (mm month $^{-1}$) ~~between~~ for a) ICON266, ~~and~~ b) ICPL266 and c) ICPL266_flx compared to the E-OBS data for the period of 2010-2018.

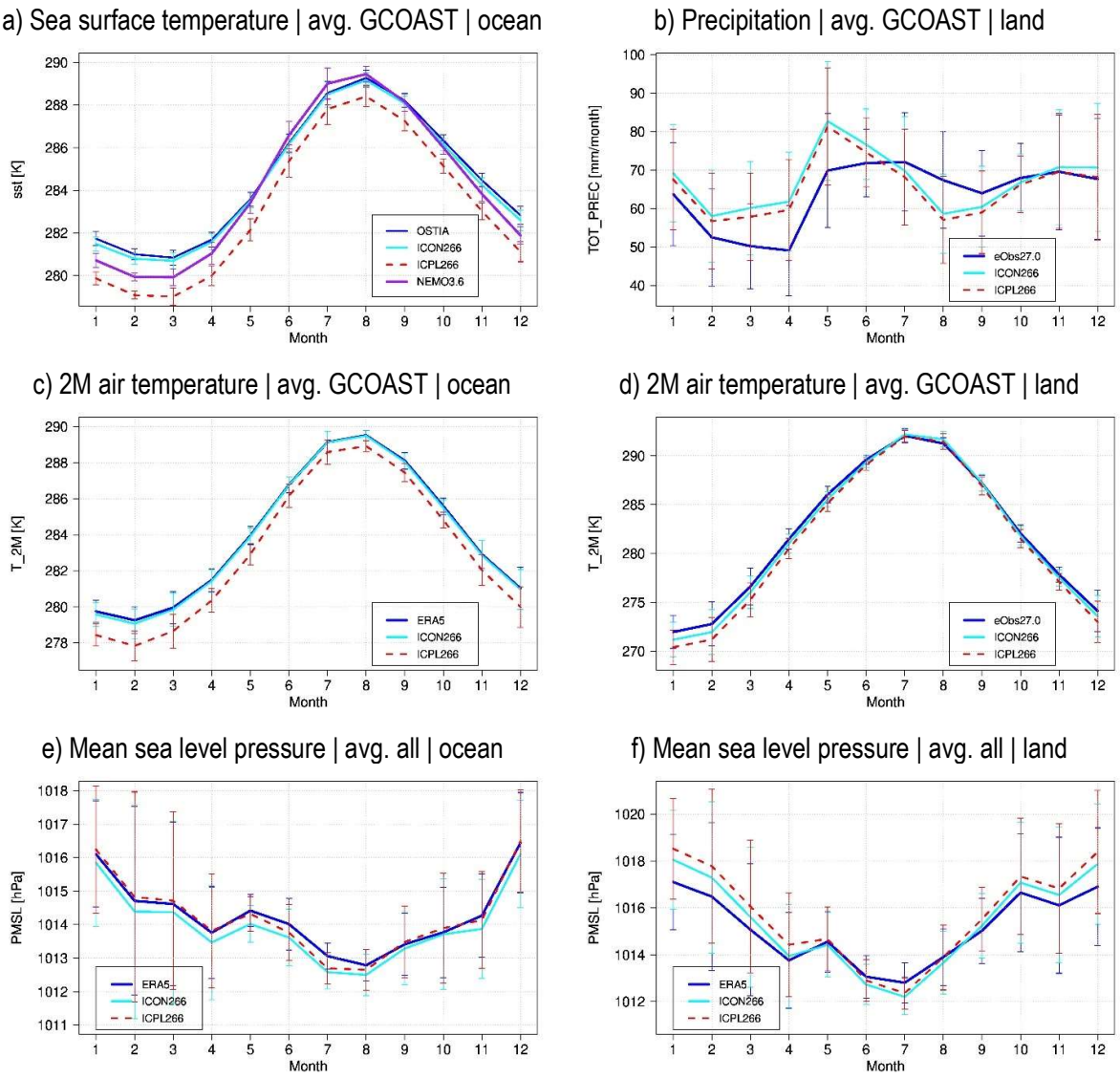

Figure 1~~0~~1: Climatological monthly mean of T_S (K), T_2M (K), PMSL (hPa) and precipitation (mm/month) of ICON266 (cyan solid line) and ICPL266 (red dashed line) compared to the OSTIA, ERA5 and E-OBS data (blue solid line) for the period of 2010-2018. a) includes also the SST of NEMO 3.6 (purple solid line) averaged over the GCOAST domain. Values are averaged over the GCOAST domain (avg. GCOAST) or the whole EURO-CORDEX domain (avg. all), over the ocean or land points only. The vertical bars show the standard deviation of the area mean data.

a) Sea ice fraction bias, ICPL266

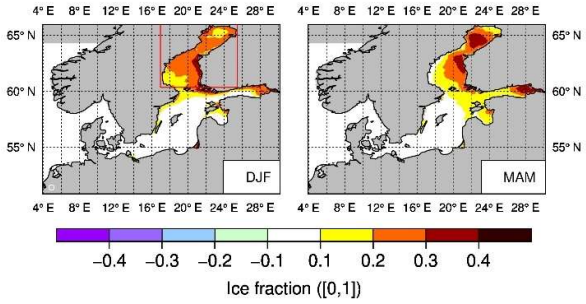

b) Sea ice fraction bias, ICPL266_flx

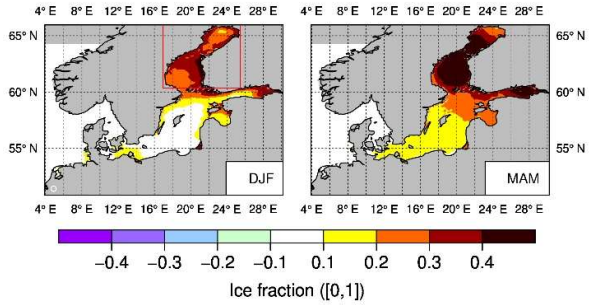

~~b) Sea ice fraction bias, NEMO3.6~~

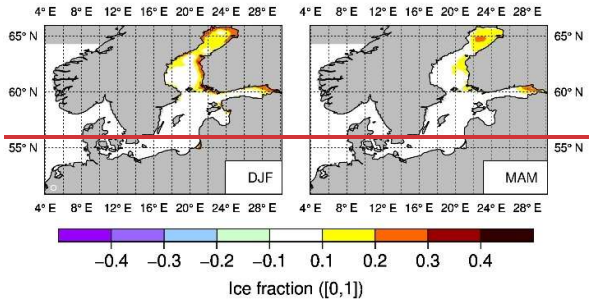

c) Sea ice fraction bias, NEMO3.6

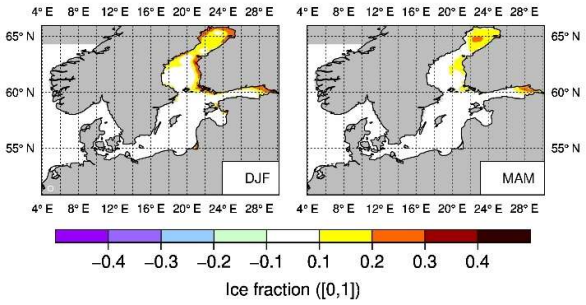

~~c~~d) Sea ice fraction, Bothnian Bay & Sea

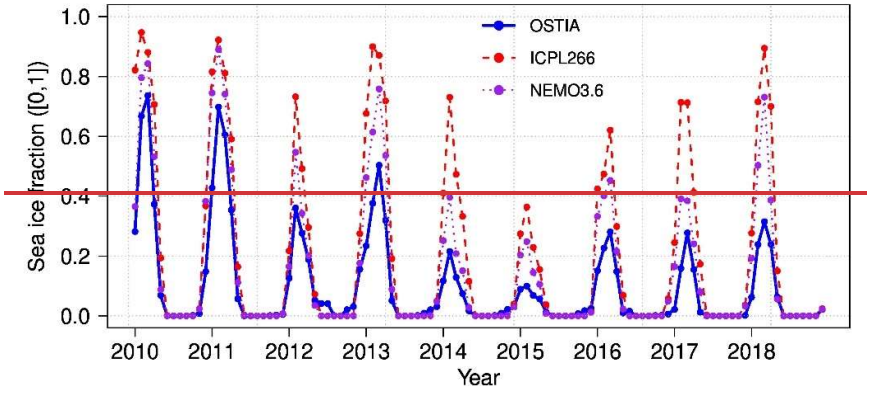

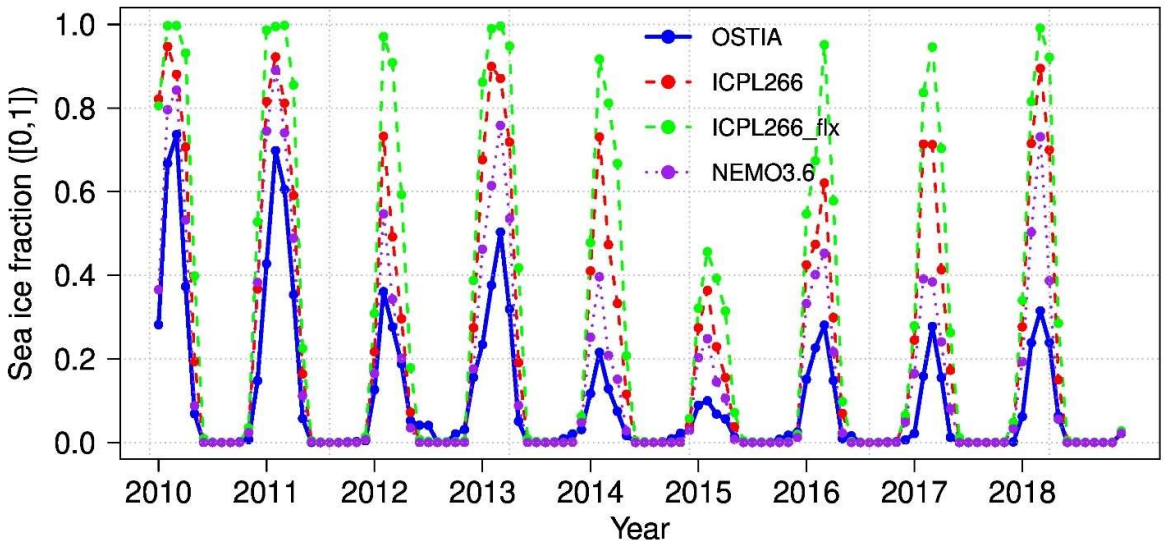

Figure 1~~2~~: Sea ice fraction bias of a) ICPL266, b) ICPL266_flx, ~~and b~~c) NEMO3.6 compared to the OSTIA data in winter (DJF) and spring (MAM) averaged over the period of 2010-2018; ~~c~~d) Monthly mean of sea ice fraction averaged over the Bothnian Bay & Sea (red box in Fig. ~~12a~~11a) of OSTIA, ICPL266, ICPL266_flx and NEMO3.6 during 2010-2018.

864

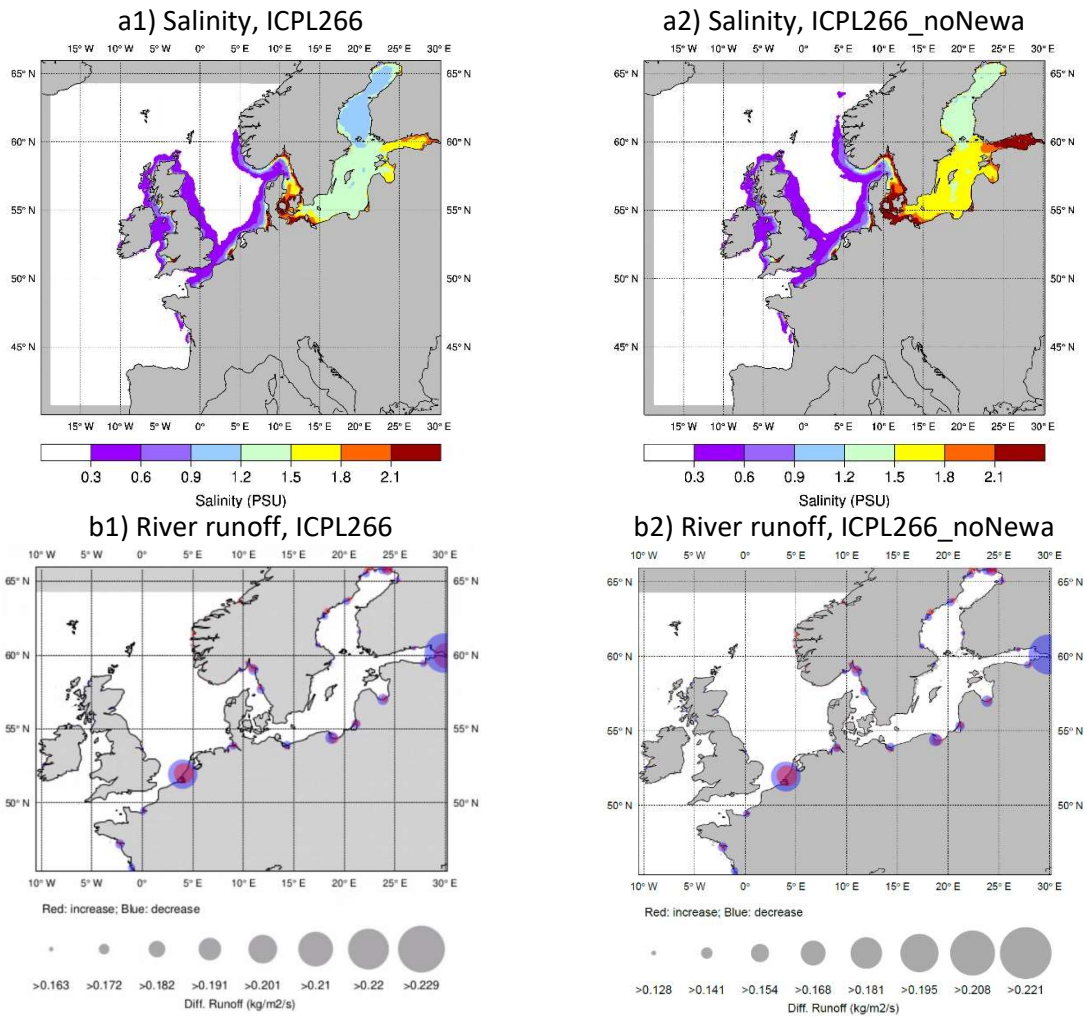

Figure 1~~2~~2~~3~~: a1) Salinity difference (PSU) and b1) river runoff difference (kg/m2/s) between ICPL266 and NEMO3.6 averaged over the period of 2010-2018. a2) and b2) salinity and river runoff difference of ICPL266_noNewa compared to NEMO3.6. In Fig. ~~13~~ 12 b1 and b2, the size of the grey circles indicates the magnitude of the positive (red color) and negative (blue) differences.

865